CHALMERS
UNIVERSITY OF TECHNOLOGY

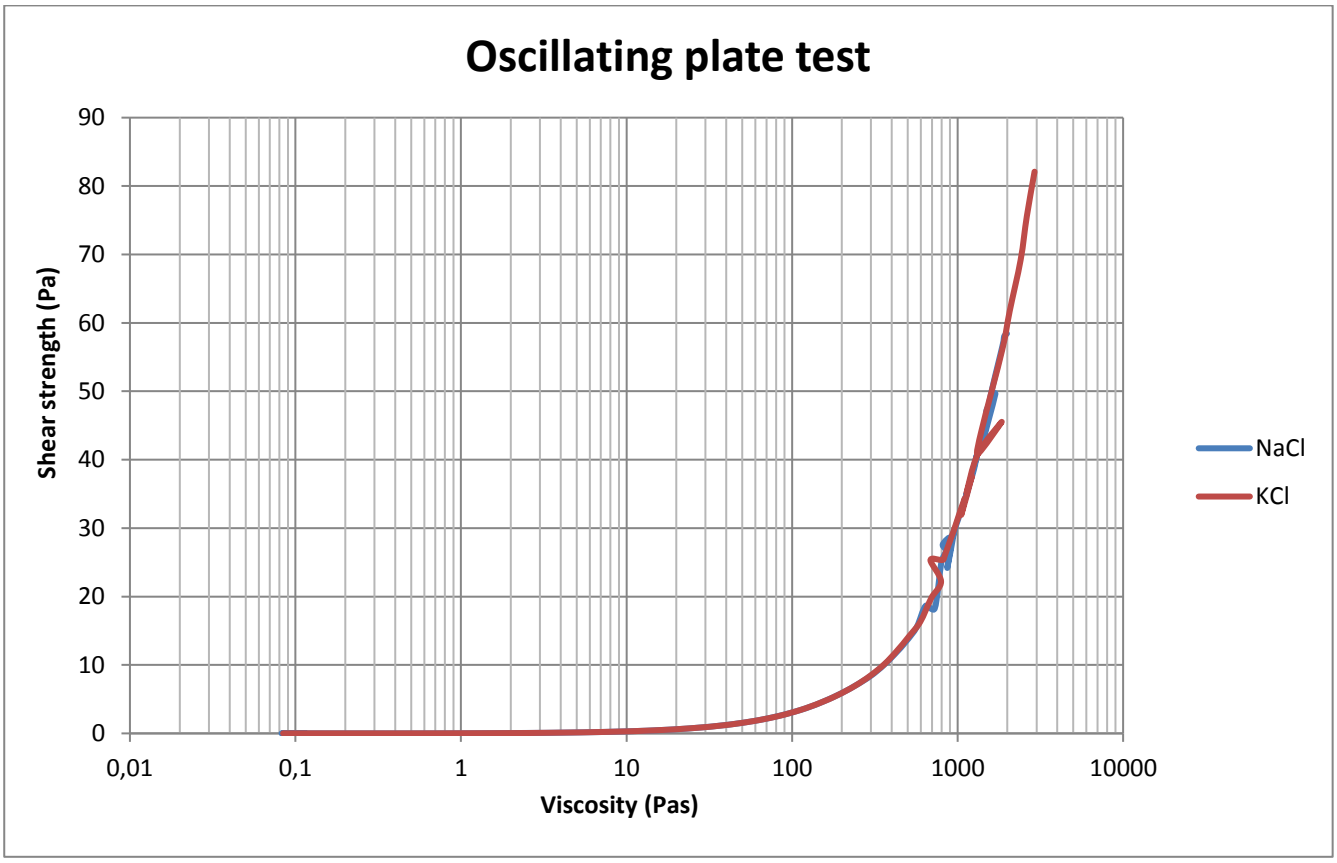

Shear strength and erosion susceptibility of silica sol

Laboratory studies of a grouting material using mechanical tests, rheological tests and a fracture replica

Master of Science Thesis in the Master's Programme Infrastructure and Environmental Engineering

FRIXOS A. LIVERIOS
ROBIN NILSSON

Department of Civil and Environmental Engineering
Division of GeoEngineering
CHALMERS UNIVERSITY OF TECHNOLOGY
Master's Thesis BOMX02-16-156
Gothenburg, Sweden 2016

MASTER'S THESIS BOMX02-16-156

Shear strength and erosion susceptibility of silica sol

Laboratory studies of a grouting material using mechanical tests, rheological tests and a fracture replica

Master of Science Thesis in the Master's Programme Infrastructure and Environmental Engineering

FRIXOS A. LIVERIOS

ROBIN NILSSON

Department of Civil and Environmental Engineering
Division of GeoEngineering
CHALMERS UNIVERSITY OF TECHNOLOGY
Gothenburg, Sweden 2016

Shear strength and erosion susceptibility of silica sol
Laboratory studies of a grouting material using mechanical tests, rheological tests and a fracture replica

Master of Science Thesis in the Master's Programme Infrastructure and Environmental Engineering
FRIXOS A. LIVERIOS
ROBIN NILSSON

Examensarbete / Institutionen for bygg- och miljöteknik
Chalmers tekniska högskola, 2016

Department of Civil and Environmental Engineering
Division of GeoEngineering
Chalmers University of Technology
SE-412 96 Göteborg
Sweden
Telephone: + 46 (0)31-772 1000

Cover: Shear strength development of two types of silica sol with respect to viscosity.

Reproservice, Chalmers University of Technology
Göteborg, Sweden 2016

Shear strength and erosion susceptibility of silica sol
Laboratory studies of a grouting material using mechanical tests, rheological tests and a fracture replica

Master of Science Thesis in the Master's Programme Infrastructure and Environmental Engineering

FRIXOS A. LIVERIOS, ROBIN NILSSON
Department of Civil and Environmental Engineering
Division of GeoEngineering
Chalmers University of Technology

ABSTRACT

The aim of this thesis is to find the shear strength development, viscosity development and erosion susceptibility for two types of silica sol – one mixed with NaCl and the other with KCl. Three types of tests have been conducted – mechanical tests, rheological tests and an erosion test using a fracture replica. The mechanical tests that were conducted were the fall cone test and the uniaxial compression test. The rheological tests involved a cup and bob setup for determining the viscosity development and an oscillating plate setup for determining the shear strength development during the gelling process. The erosion test was performed by grouting a fracture replica with silica sol and observing if the stress from the water was enough to erode the grout. The results show that the shear strength of the silica sol at gelling is in the range of 60-80 Pa, while the shear strength after five days varies between 20-23 kPa, with the fall cone test giving higher values than the uniaxial compression test. The viscosity was found to increase exponentially over time and the viscosity development was identical for both accelerators. The shear strength of both types of silica sol was found to increase exponentially with viscosity. Further, the erosion test shows that silica sol is capable of withstanding the stress due to water pressure in a fracture. For all tests KCl was found to give a higher shear strength than NaCl. However, the difference is slight and seems to only occur after gelling.

Key words: silica sol, gelling liquid, grouting, shear strength, viscosity, erosion, fracture replica, oscillatory rheology, oscillating plate test.

Table of Contents

Preface

The work presented in this thesis was performed at the Department of Civil and Environmental Engineering, Division of GeoEngineering at Chalmers University of Technology, Sweden. The work has been carried out from January 2016 to June 2016. Christian Sögaard has acted as supervisor for this project and Johan Funehag has acted as the examiner.

We, the authors, would like to express our gratitude to everyone who has contributed to this Master's thesis project. We would like to thank our supervisor Christian Sögaard for all the support and the feedback he has given as well as for his help with the lab work. We would also like to thank our examiner Johan Funehag for challenging us throughout this project and giving us new perspectives to consider. Many thanks also to Peter Hedborg for his help with the mechanical tests, Aaro Pirhonen for helping us with setting up our test equipment and to Mona Pålsson for her guidance and supervision during the work we have performed in the WET lab. Finally, we would like to express our thanks to Henrik Persson and Mats Larsson at Malvern Instruments for their help with planning the oscillating plate test.

Göteborg, June 2016

Frixos A. Liverios

Robin Nilsson

Notations

Roman upper case letters

A	[m^2]	Cross-sectional area
C	[1/ms]	Constant
L	[m]	Length
W	[m]	Width

Roman lower case letters

b	[m]	Hydraulic aperture
g	[m/s^2]	Gravity acceleration
h	[m]	Pressure head
k_β	[-]	Constant based on cone angle
m	[kg]	Mass
m_{load}	[kg]	Load weight
n	[-]	Critical exponent
z	[m]	Elevation head

Greek upper case letters

ΔH	[m]	Loss of head

Greek lower case letters

α	[-]	Constant
β	[Degrees]	Cone angle
γ	[-]	Shear strain
γ_0	[-]	Shear strain amplitude
δ	[Rad]	Phase shift
μ_0	[Pas]	Initial viscosity
μ_g	[Pas]	Viscosity of grout
μ_w	[Pas]	Viscosity of water

ρ_w	[kg/m^3]	Density of water
σ	[Pa]	Compressive strength
τ	[Pa]	Shear strength
τ_u	[Pa]	Undrained shear strength
τ_{grout}	[Pa]	Shear strength of grout
τ_{water}	[Pa]	Shear stress of water
ω	[Rad/s]	Oscillation frequency

Mathematical expressions

$G'(\omega)$	[Pa]	Storage modulus
$G''(\omega)$	[Pa]	Loss modulus
$\Delta H/L$	[-]	Hydraulic gradient

Abbreviations

TDS	Total Dissolved Solids

1. INTRODUCTION

During the construction of underground structures that take place below the groundwater table (e.g., tunnelling), it is very important to consider the water inflow that might occur. In such cases, the most conventional method to reduce the groundwater leakage is called grouting. The groundwater inflow can cause several complications both in the working site and the surrounding environment. Some of the most serious consequences regarding lowering of the groundwater can be ground settlements (especially in building/residential areas), drying of wells, drying of vegetation and rotting of wooden piles under certain constructions. The grouting process is primarily effective at medium depths. At great depths, where water inflow can be considerably high, the grouting method can be challenging and unsuccessful. If this is the case, several post grouting processes have to be done, ensuing higher construction costs and critical delays.

The main reason for the different complications in underground constructions, is the water pressure gradient that acts against the site area. To avoid any water ingress, the grout agents have to resist the water force and flow that derives from the water pressure gradient. It is important here to note that the initial grouting stage is of great importance, due to the lower strength development of the used grouting material. In order to clearly understand the process, numerous experiments and evaluations have to be conducted regarding the acting water forces and the grouting agents' strength. There is an increasing trend lately regarding underground constructions in urban areas as well as the building of tunnelling structures in great depths. Therefore, it is important to thoroughly examine these processes and find effective, sound and sustainable solutions (Axelsson, 2006).

The most common grouting materials are the fine-grained cementitious grouts. These materials can penetrate fractures as small as 0.1 mm, but the requirements of inflow of water into tunnels have increased in the last decade (Funehag, 2005). Although they demonstrate a high final strength, their initial strength can be characterized as mediocre. Regarding their penetrability properties, these grouts can prove ineffective against rock with low conductive and very narrow fractures. In such occasions, non-cementitious grouts can be used. These types of grouts demonstrate a fast initial strength development but they lack in final strength compared to cementitious grouts. A grouting agent that will be used to seal fractures in hard rock has to meet the relevant demands and be able to withstand the water force. Due to the lack in final strength, a non-cementitious grout might not be able to cope with these requirements (Axelsson, 2006).

Chemical (or non-cementitious) grouts can penetrate narrow fractures (silica sol can penetrate very narrow fractures, 0.01 mm in aperture). However, due to the risk of harming the surrounding environment including posing health risks for human beings, they should be used with caution, depending on the grouting agent (Butrón, 2005).

Even today, chemical grouts are not commonly used in order to control water ingress to tunnels and this is partially due to lack of knowledge and experience concerning environmental risks and partially due to little knowledge regarding longtime strength of the

material. However, silica sol is a chemical grout with increased use as a grouting agent during recent years.

Silica sol has been introduced to the market due to the need for environmentally friendly materials for grouting purposes. The material is composed of a suspension of silica nanoparticles that create a gel when mixed with an accelerator (usually a salt). The benefits of silica sol as a grouting agent are many. The material is nontoxic, making it environmentally friendly. It can also effectively penetrate and seal narrow fractures that would be impossible to grout using conventional cementitious grouts. Lastly, the low pH of silica makes it especially interesting for nuclear waste repositories, where the high pH of cement is an undesirable property.

Despite the benefits of silica sol as a grouting material, little research has been done on its properties. If silica sol is to see widespread usage within grouting applications, more research must be done in order to ascertain the suitability of the material (Butrón, Axelsson and Gustafsson, 2007).

1.1. Aim, objectives and scope of work

The aim of this project is to investigate the shear strength development and erosion susceptibility of silica sol in grouting applications. The main objectives are

- Finding the shear strength development of silica sol, both during the gelling process and for a period of five days after gelling
- Finding the viscosity development of silica sol during the gelling process
- To establish the relationship between shear strength and viscosity
- To investigate how the choice of accelerators affects the material
- To investigate if the silica sol is capable of resisting the erosion due to stress from the water in a fracture.

To achieve these objectives, laboratory studies of silica sol were conducted using mechanical and rheological tests as well as a fracture replica. The mechanical tests that were performed are fall cone and uniaxial compression tests, in order to find the long-term shear strength. The rheological tests aim to find the short-term shear strength and viscosity of the material. These tests were conducted using a rheometer and two types of test setup – a cup and bob setup and an oscillating plate setup. The fracture replica was used to allow for subjecting the silica sol to the water stresses present in a fracture in order to ascertain if the material will erode.

This project is limited to the study of one type of silica sol (Meyco MP 320) and two types of accelerators (NaCl and KCl). The effect of different environments on the material is outside the scope of this project. However, basic control of temperature and humidity has been performed.

2. LITERATURE REVIEW

2.1. Mechanical properties

This section deals with studies of the mechanical properties of silica sol, such as shear strength, compression strength and hydraulic conductivity, to name a few. A broad understanding of the material properties of silica sol has been sought, with a focus on understanding the behaviour of the shear strength as well as test methodology. Where applicable, the sample composition and the type of silica sol used have been mentioned.

A study conducted by Axelsson (2006) deals with the mechanical properties of silica sol in different environments. The samples were stored at 8 °C in three different relative humidities – 75, 95 and 100 %. While the type of silica sol was not mentioned, the specifics of the mix can be seen in table 1. The tests were conducted during a six-month period were the samples were tested for drying shrinkage, compressive strength, Young's modulus, shear strength and flexural strength. The compressive strength was measured using the European Standard for hardened concrete, while Young's modulus was determined from the assumption that silica sol acts as an elastic material. Shear strength measurements were conducted using a fall-cone test. Finally, flexural strength was measured using the European Standard for flexural strength of hardened concrete.

Table 1 – Silica sol mix used in Axelsson (2006).

Concentration of silica (% by weight)	35 %
Concentration of $CaCl_2$ in accelerator (% by weight)	2.9 %
Concentration of aluminium (% by weight)	0.26 %
Ratio of silica sol to accelerator	8:1
pH	10

The results from Axelsson (2006) show that the strength (compressive, shear and flexural) and modulus of the silica sol increases over time, with the largest increase occurring after 1000-3000 hours. The results also show that most of the drying shrinkage occurs 200-1000 hours. In general, a lower relative humidity leads to a greater increase in strength and more drying shrinkage. The failure mode for silica sol is at first ductile, but becomes more brittle as strength increases. Finally, the author found that while modelling silica sol using the Mohr-Coulomb failure criterion, the friction angle increased from 20° to 50° during the six-month study period.

As a follow-up on the work conducted by Axelsson (2006), Butrón, Axelsson and Gustafson (2007) conducted an extensive collection of tests in the mechanical properties of silica sol. The tests conducted were unconfined compression, fall cone, consolidated and unconsolidated undrained triaxial, oedometer, continuous water loss, water loss with varied humidity, drying out between transparent plates and diffusion of chlorides into the silica sol. The samples for the tests were stored in a number of environments with varying temperature and humidity,

with some of the samples stored in high pH or with a high concentration of total dissolved solids (TDS). The temperatures ranged from 8-60 °C and the humidity from 75-100 %. A high pH was defined as pH 11, while a high concentration of TDS was defined as 35 g/L. Some of the samples were also stored immersed in water. The type of silica sol used in these experiments was Eka Gel EXP36. The results from this study shows that the strength of the silica sol increases with time, especially in low humidity and high temperature environments. A thin layer with low shear strength was found to emerge at the contact surface between the silica sol and the water. When scraped off, the authors found that a new layer will not be formed. The authors also found that the silica sol displays a vertical failure plane during the unconfined uniaxial compression tests. Further observations made by the authors indicates that the silica sol is susceptible to drying shrinkage and that the fracture behaviour for silica sol goes from ductile to brittle when exposed to drying. Finally, the authors conclude that silica sol is not under any risk of shrinking when used in grouting applications, since the diffusion of water into the silica from the groundwater in a fracture is enough to prevent any significant shrinkage.

Further building on the body of work already presented, Butrón, Axelsson and Gustafson (2009) performed a number of tests on silica sol with the intention of understanding its behaviour as a grouting material in hard rock. The properties tested were strength, fracture behaviour and hydraulic conductivity and the properties were tested using fall-cone, triaxial shear, unconfined compression and oedometer tests. Like in the previous study from Butrón, Axelsson and Gustafson (2007), the samples used were stored in different environments with varying humidity, temperature and chemical surrounding. The temperatures ranged from 8-60 °C, the humidity from 75-100 % (with some samples being immersed) and the chemical environments used were deionized water, high TDS and pH 11. All the samples were tested during a period of 5 months. A single type of silica sol, Eka Gel EXP36, was used for all the samples as in the previous study. The results are consistent with those found in Butrón, Axelsson and Gustafson (2007) and show that the strength of the silica soil increased over time in all the samples and that the shear strength depends largely on the environment during gelling. High pH and low temperature seems to have the greatest negative effect on the strength development. The results found that shorter hardening times lead to greater axial compression. For samples tested at 29 days and 64 days after gelling, failure occurred at 27 and 33 kPa, respectively. For samples tested during the first 13 days no failure occurred at 20 kPa axial stress. It is curious to note that the silica sol stored in water or in high pH developed a thin layer with low shear strength. However, this layering effect did not significantly affect the shear strength of the samples. The authors conclude that silica sol performs satisfactory in all the tested environments and that the shear strength of hardened silica sol is adequate for normal conditions.

Persoff et al. (1997) studied the effect of dilution and contamination on the strength of sand grouted with silica sol. The project was divided into four steps. First, samples of Monterey sand were grouted with silica sol that had been diluted in a variety of ways, so that the contents of colloidal silica ranged from 4.9 % to 27 %. Second, the unconfined compression strength and the hydraulic conductivity were measured. Third, samples without contaminants

were prepared and then immersed in contaminant liquids. The silica sol used was DuPont Ludox SM. The unconfined compressive strength was measured according to the ASTM C-39-86 standard. The results show that the unconfined compression strength of sand grouted with silica sol increases with the content of silica in the grouting material. The authors reason that this behaviour is due to the cohesive effect of the silica, as the sand itself would not have an unconfined compressive strength. This suggests that colloidal silica can bind to silica found in other materials. The authors also found that immersion in water slows the strength gain, while immersion in water by contaminated aniline can weaken the silica sol. However, the other contaminants in the study had no statistically significant effect on the long-term strength of the silica sol.

In another study conducted by Persoff et al. (1998), a number of samples of silica sol were tested for a construction project at the Savannah River. The requirements for the grouting material were low initial viscosity, low permeability when gelled, no requirement of excessive pressure for injection and a controllable gel time. Three samples of silica sol and brine (see table 2 for the properties and composition of the samples) were tested for pH, viscosity and content of solids. The samples were also tested for gel time with and without soil, by placing the silica in a jar and slowly adding the appropriate amount of brine. The mixture was then allowed to sit between measurements. Drain-in tests were used to screen out silica that might react with the soil to cause gelling. This test is conducted by packing soil in a vertical column and the pouring colloidal silica, without brine, into the soil column. The amount of colloidal silica that runs through the column determines its propensity to gel in contact with soil. Column tests, where two tests are performed in sequence in a column of packed soil, were performed to establish the required injection pressure and rate at which the grout gels in the soil. Column injection tests were performed to measure the hydraulic conductivity, while column gel-time tests were performed to measure gel time. Finally, drips tests were performed as an additional method of measuring gel time.

Table 2 – Properties and contents of the silica sol samples (Persoff et al., 1998).

Sample	**1**	**2**	**3**
Stabilizing agent	Alumina coating	High pH, Na counter ion	Alumina coating
Particle charge	Negative	Negative	Negative
Average particle diameter	14 nm	7 nm	8 nm
Density, g/cm^3	1.21	1.22	1.17
Silica content	30 %	30 %	25 %
NaOH content	n/a	0.56 %	0.40 %
pH	7	10	7
Brine	$CaCl_2$	NaCl, $MgSO_4$, citric acid	$CaCl_2$

The results from Persoff et al. (1998) that the viscosity criteria and the permeability criteria are both satisfied for all three samples. The requirement for the viscosity was below 10 mPas, with the samples ranging from 4.23 mPas to 7.85 mPas. The requirement for the permeability was a hydraulic conductivity of less than 10^{-8} cm/s, with the samples falling in the range of $0.4\text{-}1*10^{-8}$ cm/s. All of the samples could be injected into the soil without premature gelation (indicating that gel times can be properly controlled). However, for the excessive grouting

pressures, the authors found some issues regarding the concentration of the brine used – if the gel time is to be reduced by increasing the concentration of brine, premature gelling may occur which may lead to too high injection pressures. In conclusion, the authors state that it is important to perform these tests on all silica sol grouts before usage in a geotechnical application to ensure the proper functioning of the material.

2.2. Viscosity development

Funehag and Gustafson (2008) have developed a method for calculating the penetration length of silica sol. Since silica sol functions differently from cementitious grouts in that it is a Newtonian liquid without a yield stress, the same methods for calculating the penetration length cannot be used for both materials. Instead, the authors suggest that the penetration length of silica sol can be calculated as both 1D channel flow and 2D radial flow (Funehag and Guftafsson, 2008). The 1D case has been modelled by the authors in two ways – one way assuming constant viscosity and the other taking into account the gelling of the silica sol. In the former, the viscosity is assumed to be constant while in the latter, the viscosity change of the silica sol is used in the equation for the penetration length. Also, for the latter case, dimensionless parameters are introduced by the authors to simplify the integrations. For the 2D case, the authors have modelled the penetration length using the results from the 1D case taking into account the gelling of the silica sol. In the 2D radial model, dimensionless parameters are introduced in a similar fashion to the 1D gelling case. When the expressions were derived, the authors did laboratory tests using pipe flow tests to validate their model. Several tests using different gel times and grouting pressures were performed. The authors also used other Newtonian liquids such as water and oil to test the model. Their results show that the model fits well for water, but underestimates the penetration length of silica sol and oil, which they reason may be due to slip at the walls of the plastic pipe. Further, the authors conclude that due to the difficulty of measuring the gel induction time, which is an essential parameter in the model, the pre-evaluated viscosity development may be used to identify a suitable gel induction time.

In this paper, the authors use the following equation to model the viscosity change of the silica sol (Funehag and Gustafsson, 2008)

$$\mu_g = \mu_0\left(1 + e^{\alpha\left(\frac{t}{t_G}-1\right)}\right)$$

where μ_g is the viscosity at a given time, μ_0 is the initial viscosity, α is a an experimentally derived constant that accounts for the hardening of the gel, t is the elapsed time and t_G is the gel induction time, which is the time at which the viscosity of the material has doubled. Using this equation, it is possible to model the viscosity as a function of time.

2.3. Erosion and hydraulic gradient

On the topic of erosion of silica sol in grouting applications, Suresh & Tohow (2013) attempted to design a grouting procedure based on the hydraulic gradient in order to prevent erosion of the grout. The authors conducted a number of field tests on a service tunnel in Gothenburg where previous grouting measures had failed. Field tests included core mapping, single and double packer natural inflow tests, water pressure tests, pressure build up tests and a test grouting to evaluate the design. With the results from these tests, the authors could calculate the shear stress of the water to 25 Pa.

Further studies on the erosion of silica sol have been conducted by Reynisson (2014). The author studied the TASS tunnel, which is part of the Äspö Hard rock laboratory, in order to evaluate the performance of the grouting having been performed in the tunnel. Part of this evaluation was the calculation of the shear stress from the water and its action upon the silica sol grout in the fractures. In order for the grout to withstand the pressure of the water, the following criteria must be fulfilled, modified from Axelsson (2009)

$$\tau_{grout} \geq \frac{\rho_w \cdot g \cdot b}{2} \cdot \left(-\frac{\Delta H}{L}\right)$$

where τ_{grout} is the shear strength of the grout, ρ_w is the density of water, g is the gravitational constant, b is the hydraulic aperture and $-(\Delta H/L)$ is the hydraulic gradient. In order to estimate the hydraulic gradient, Reynisson used four methods – theoretical, simplified, worst case and according to geometry. The theoretical method used mathematical models to calculate the hydraulic gradient for three cases – after pre grouting, after post grouting and current. The simplified method involves measuring the pressure loss from the grouting packer to the borehole opening, while the worst case scenario assumes that the fracture with the highest flow is located at the place of the packer. Finally, the gradient according to geometry, the fracture network was obtained from the geological mapping of the TASS tunnel and the water bearing fractures were identified, allowing for the gradient to be calculated. The average hydraulic gradients for methods simplified, worst case and according to geometry were found to be 26, 51 and 51 m/m, respectively. For the three cases in the theoretical method, after pre grouting, after post grouting and current, the theoretical hydraulic gradient was found to be 231, 52 and 51 m/m, respectively. Table 3 shows the results for the shear stress of water for the methods simplified, worst case and according to geometry.

Table 3 – Shear stress of water for three methods (Reynisson, 2014).

Method	Average (Pa)	Minimum(Pa)	Maximum (Pa)
Simplified	5	0	37
Worst case	10	0	66
According to geometry	13	1	64

While the work done by Reynisson is valid only for a specific location, it is still of interest to this thesis since it offers a number of possibilities for calculating the shear stress of water. This is important for the erosion test, where the shear stress of water must be known.

2.4. Rheology

Soft materials like foams, emulsions and dispersions can be found everywhere in formulations and industrial products. These materials show some distinctive mechanical behaviour. Their response to any stress or force is viscoelastic, which can be defined as an intermediate state between liquids and solids. Consequently, studying the mechanical behaviour of these materials can be quite complicated. Viscometry and oscillatory rheology can be characterized as typical experimental tools for studying such behaviour. It provides new insights about the physical mechanisms that govern the unique mechanical properties of soft materials.

Rheology studies deformations and flows of materials. Deformation is defined as the strain while flow as the strain rate; it is the distance over which a body moves under the effect of an external force (stress). Accordingly, rheology is considered as the stress-strain relationships analysis in materials. The measurement of rheological properties is applicable to all materials – from fluids such as dilute solutions of polymers and surfactants through to concentrated protein formulations, to semi-solids such as pastes and creams, to molten or solid polymers as well as asphalt (Malvern Instruments, n.d.)

A rheometer is a precise apparatus that encloses the material sample in a geometric arrangement, adjusts the surrounding environment, while also applying and measuring extensive ranges of stress, strain, and strain rate.

The different material behaviours to strain and stresses vary from purely elastic and purely viscous to a combination of those, known as viscoelasticity. These behaviours are quantified in material properties such as modulus, viscosity, and elasticity (see figure 1). Many frequently used materials demonstrate important complexity regarding their rheological properties, whose viscosity and viscoelasticity can be miscellaneous, depending on the external effects such as stress, strain, temperature and timescale (TA instruments, n.d.).

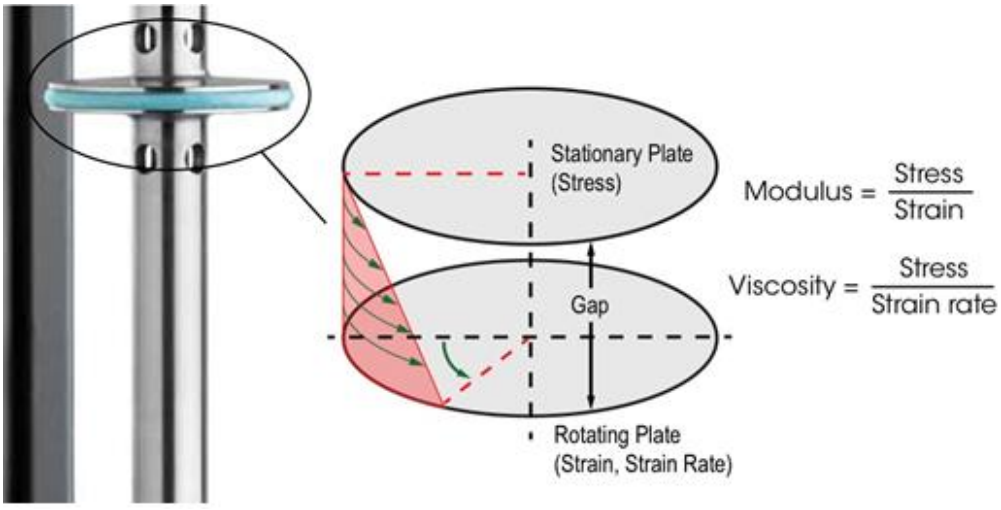

Figure 1 – Stress-strain relationship in material (TA Instruments, n.d).

2.4.1. Cup and bob viscometry

A viscometer or viscosimeter is an apparatus that can measure the viscosity and the flow parameters of a fluid. However, viscometers are able to take measurements only under one flow state. In order to measure the diverse viscosity of liquids with fluctuating flow conditions, a rheometer has to be used. Cup and bob viscometer is a set-up that can be used together with a rheometer instrument and measure the viscosity of such liquids.

The concept behind the rotational viscometer is that the required force to rotate an object in a fluid can work as an indicator of the viscosity of that fluid. Consequently, the required force to rotate a bob in a fluid at known speed can be determined by this apparatus. The objective of the cup and bob viscometers function is to define the exact sample volume that has to be imposed into shear stresses within a test cell. In parallel, measurements that estimate the required torque to achieve a certain rotational speed are taking place.

There are several types of cup and bob measuring systems. These can be the double gap, the Mooney cell or the DIN coaxial cylinder systems (figure 2).

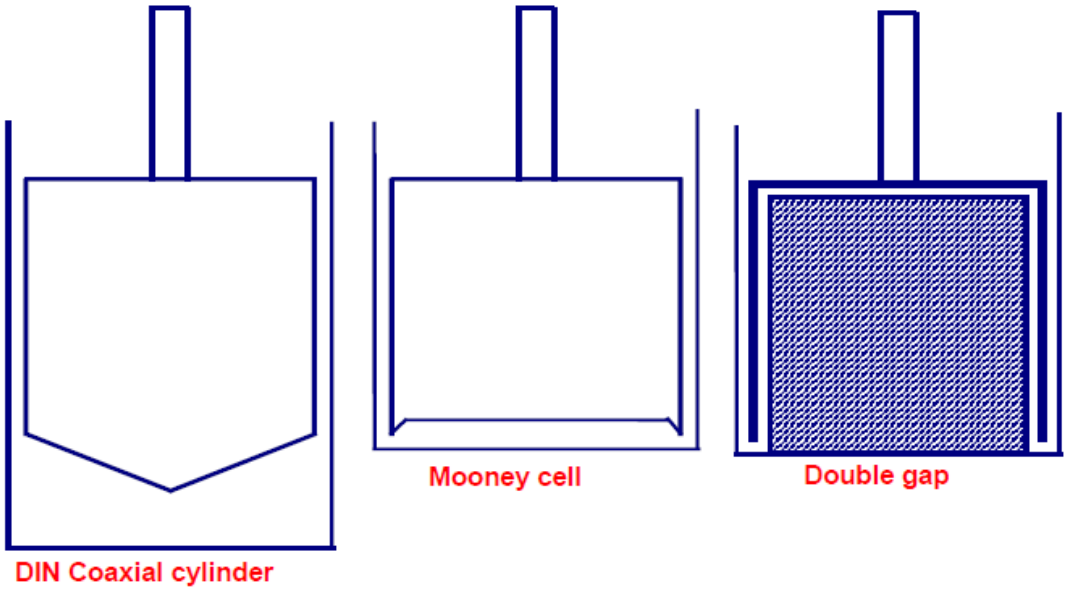

Figure 2 - DIN Coaxial cylinder, Mooney cell and double gap cup and bob measuring systems (Bohlin Instruments, 1994).

The DIN coaxial cylinder is defined by the diameter of the inner side of the bob. For example, a C25 coaxial 'Cup and bob' consists of a 25 mm diameter bob, while the cup diameter is in proportion to the bob dimensions. On the other hand, double gap systems are usually defined by both the outer and the inner diameters (e.g. DG 40/50) (Bohlin Instruments, 1994).

There are two typical coaxial cylinder cup and bob arrangements – the Searle system and the Couette system. For the Searle system, the cup (outer cylinder) remains stable while the bob

(inner cylinder) rotates with a pre-set speed and the torque required to sustain this speed is measured. For the Couette system, the bob remains stable and the cup rotates at a constant rate, while the torque of the inner cylinder is estimated. As can be seen in figure 3, the space between the two vertical coaxial cylinders is filled with the liquid that is being tested (Kyoto Electronics Manufacturing, 2014).

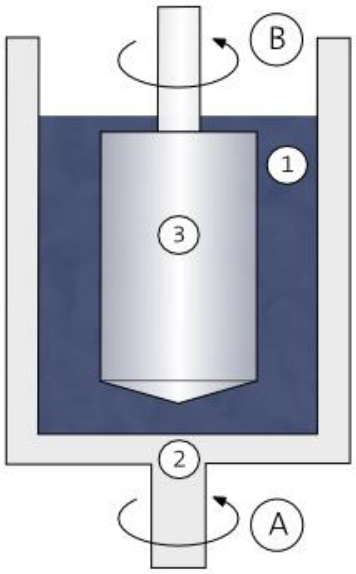

Figure 3 - Couette (A) and Searle (B) Cup and bob systems illustration, where 1 is the liquid sample, 2 is the cup and 3 is the bob (Kyoto Electronics Manufacturing, 2014).

Considering the disadvantages when using cup and bob systems, they generally require rather large amounts of samples, while they are difficult to get cleaned. In addition, due to their large mass and inertias, complications can appear during high frequency measurements.

However, cup and bob geometries can operate well with low viscosity materials or mobile suspensions. Moreover, their high sensitivity makes them capable of generating reliable data at low viscosities and shear rates.

In addition, some materials are susceptible to a skinning effect after some time, mostly due to evaporation processes. A solvent trap can be used along with the measuring system in order to overcome this obstacle. Likewise, another method would be to add a very low viscosity silicon oil layer on the top of the sample in the cup. Assuming that the sample and the silicon oil are not miscible, this solution can prove to be especially efficient (Bohlin Instruments, 1994).

2.4.2. Oscillatory rheology

Oscillation testing can be characterized as the most common test type for assessing the properties of viscoelastic materials. The viscoelastic parameters can be measured as a function of deformation amplitude, frequency, time, and temperature.

The basic principle of an oscillatory rheometer is to induce a sinusoidal shear deformation in the sample and measure the resultant stress response. The oscillation frequency ω of the shear deformation, determines the time scale. During the experiment procedure, the specimen is placed between two plates, see figure 4 (a). The bottom plate rotates, while the top plate remains stationary, and hence a time dependent strain $\gamma(t) = \gamma\sin(\omega t)$ is imposed on the specimen. By measuring the torque that the sample exerts on the top plate, the time dependent stress (t) is calculated.

Significant differences between the materials are illustrated after measuring the time dependent stress response at a single frequency, see figure 4 (b). When the material is an ideal elastic solid, then the specimen stress is proportional to the strain deformation, and the proportionality constant is the shear modulus of the material. The stress is always exactly in phase with the applied sinusoidal strain deformation. On the contrary, the stress in the sample is proportional to the rate of strain deformation, if the material is a purely viscous fluid. Here the proportionality constant is the viscosity of the fluid. The applied strain and the measured stress are out of phase, with a phase angle $\delta = \pi/2$, as shown in the center graph in figure 4 (b).

As shown in the bottom graph of figure 4 (b), viscoelastic materials demonstrate a reaction that comprises both in-phase and out-of-phase contributions. These contributions show the extents of solid-like (red line) and liquid-like (blue dotted line) behaviour, see figure 4 (b). Accordingly, the total stress response (purple line) express a phase shift δ considering the applied strain deformation that lies between that of liquids and solids ($0<\delta<\pi/2$). The system's viscoelastic behaviour at ω is characterized by the storage modulus, $G'(\omega)$, and the loss modulus, $G''(\omega)$, which characterize the solid-like and fluid-like contributions to the measured stress response respectively. For a sinusoidal strain deformation $\gamma(t) = \gamma_0\sin(\omega t)$, the stress response of a viscoelastic material is given by

$$\tau(t) = G'(\omega) \cdot \gamma_0 \cdot \sin(\omega t) + G''(\omega) \cdot \gamma_0 \cdot \cos(\omega t)$$

In general, in a routine rheological test, the aim is to measure $G'(\omega)$ and $G''(\omega)$. Due to the time dependence of the solid-like or liquid-like state of the soft material, the measurements are made as a function of the frequency (G.I.T. Laboratory Journal, 2007).

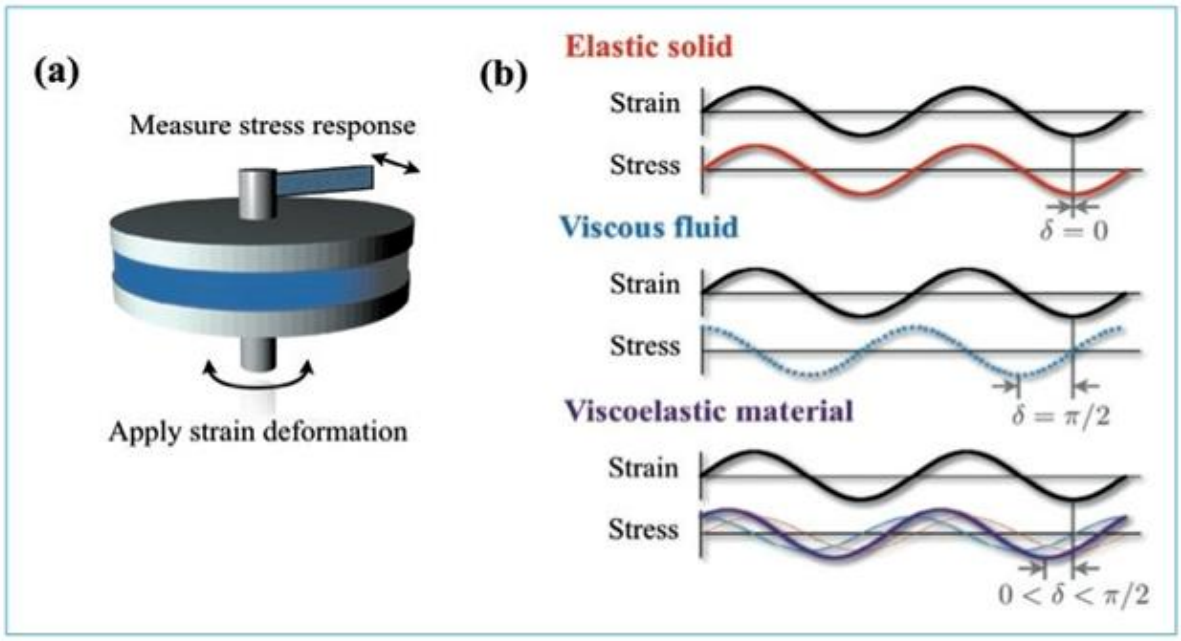

Figure 4 – (a) Schematic representation of a typical rheometry setup, with the sample placed between two plates. (b) Schematic stress response to oscillatory strain deformation for an elastic solid, a viscous fluid and a viscoelastic material (G.I.T. Laboratory Journal, 2007).

The main advantage of oscillatory tests over the rotational experiments is that they are considered to be non-destructive, when performed in the linear-viscoelastic range. More specific, during the experiment, there is no disturbance of the microstructure of the specimen by the applied forces. Consequently, oscillatory test is a more preferable process in order to assess the mechanical behaviour of complex materials. Moreover, with oscillatory tests, curing processes, phase transitions and crystallization can be examined. However, dynamic oscillatory tests require rheometers with low instrument inertia, low-friction bearing system and a very dynamic motor concept (Schramm, 2004).

As mentioned above, different measurements become available when an oscillatory excitation force is applied to a sample. To sum up, these measurements include:

Oscillatory Amplitude Sweep: The frequency of the exciting sinusoidal signal (stress or deformation) is kept constant. In parallel, the amplitude is increased progressively until the microstructure fails and the rheological material functions are not independent of the set parameter. Amplitude sweeps are mostly used to define the material's linear-viscoelastic range, but they can also be used to acquire a yield stress.

Oscillatory Frequency Sweep: The frequency is decreased or increased progressively, while the amplitude of the exciting sinusoidal signal (stress or deformation) is kept constant. Frequency sweeps demonstrate if a specimen acts like a viscous or viscoelastic fluid, a gel-like paste or fully cross-linked material.

Oscillatory Time Sweep: Frequency and amplitude of the exciting sinusoidal signal (stress or deformation) are held constant, while at the same time the material properties are monitored.

Time sweeps are used to study the various structural changes that may arise during drying and relaxation processes or gelling and curing reactions.

Oscillatory Temperature Sweep: Amplitude and frequency of the exciting sinusoidal signal (stress or deformation) are kept constant while there is an alteration in the temperature (increase and decrease). In addition, the thermal expansion of the measuring geometry that takes place during this experiment requires an automatic lift control (Schramm, 2004).

To conclude, oscillatory rheology is a valuable tool for studying the mechanical behaviour of soft materials. It may be used to determine the strength and stability. Over a given frequency range, It gives a clear indication of the behaviour of the sample, whether it performs like a viscous or viscoelastic fluid. The different results allow identification of linear- and non-linear-viscoelastic behaviour of various materials. Frequency sweeps in the linear-viscoelastic range reveal details of the microstructure for the given material and permits inferences about stability and shelf life to be concluded. In addition, oscillatory test methods can be used to monitor several liquids to solid phase changes like curing reactions and others.

Reviewing some of the research done in the field of oscillatory rheology, as it pertains to silica sol, two studies are of interest – namely, the works of Winter & Chambon (1986) and Ågren & Rosenholm (1998). In the first study, the viscoelastic behaviour of polymers was studied using oscillating tests. The authors found that at the gel point – that is, the point at which the polymer transitions from a liquid state into a solid state – occurred when $G'(\omega) = G''(\omega)$. The second study, by Ågren and Rosenholm, support this observation. In this study, the authors focused on determining how different concentrations of polyethylene glycol (PEG) affects the gelling reaction of tetraethylorthosilicates in acidic media. The authors confirmed that $G'(\omega)$ and $G''(\omega)$ are proportional to ω^n at the gelation point – a phenomena called the viscoelastic scaling law. The study also found that the value for the critical exponent n ranged from 0.71 to 0.83 for tetraethylorthosilicates.

3. METHODOLOGY

3.1. Determining the gel time

In order to ensure reliable results for the mechanical, oscillating and fracture replica tests it is necessary that the silica sol mix is consistent for all the experiments. One of the parameters that needs to be controlled is the gel time. In order to guarantee a constant gel time, the concentration of accelerators needs to be determined. The purpose of this section is to present how the visual method was used to find the necessary concentrations to give a 20 minute gel time for the silica sol.

For this experiment, the silica sol used was Meyco MP 320 and the accelerators were KCl and NaCl. The first step is to prepare the salt solutions. Two samples of 2 M salt solution – one for each salt – was prepared by mixing the required amount of salt (74.54 g of KCl and 58.44 g of NaCl respectively) in 0.5 l of deionized water and shaken until the salts were completely dissolved. Once the salt solutions were prepared, the following steps were undertaken:

1. Pour 20 ml of silica sol into a plastic test tube with a screw on cap using a micropipette.
2. The required amount of salt is added to the silica sol using a micropipette.
3. The cap is sealed and the mixture shaken for a few seconds.
4. Start the timer as soon as the mixture has been shaken.
5. Gently shake the mixture once every minute to check the viscosity.
6. Note the time at which the mixture no longer flows. This is the gel time.
7. Adjust the amount of salt solution and repeat the experiment until a 20 min gel time is observed.

The initial amount of salt solution used was 5 ml for both salts. The experiment was ended for any iteration resulting in a gel time exceeding 22 minutes. Gel times were recorded with half minute accuracy, and a half minute deviance from the goal of a 20 min gel time was allowed.

3.2. Mechanical tests

This section contains the test procedures for the mechanical tests. The aim of the mechanical tests is to find the shear strength of the silica sol. The two types of mechanical tests that have been performed are the fall cone test and the uniaxial compression test.

3.2.1. Fall cone test

The fall cone tests were performed in intervals, with the first test being performed 1 hour after gelling and subsequent tests performed every 24 hours after for a full work week, Monday to Friday. A total of 10 samples, five for each accelerator, were prepared on the first day of the

test week. The samples for the fall cone test were stored in room temperature with a small amount of water covering the silica sol in each sample to prevent drying. The samples were sealed using duct tape to further prevent drying. All samples were contained 70 ml silica sol and 16 ml NaCl or 8 ml KCl. Each sample was stirred using magnetic stirring.

1. A sample of silica sol gel is prepared in a cylindrical hard plastic cup with an inner diameter of 50 mm and a height of 45 mm (see figure 5).
2. The sample is placed in the fall cone apparatus (see figure 6).
3. A steel cone is placed into the apparatus so that the tip of the cone just touches the sample (see table 4 for cone specifications).
4. The cone is released into the sample and the immediate penetration is noted.
5. The undrained shear strength is determined using the formula $\tau_u = k_\beta \left(\frac{mg}{d^2}\right)$, modified from Hansbo (1957), where m is the mass of the cone, g is the gravitational acceleration, d is the penetration depth and k_β is a factor depending on the cone angle (see table 4 for values for m, β and k_β).

Table 4 – Cone specifications

Cone	***m***	***β***	k_β
1	10 g	60°	0.25
2	60 g	60°	0.25
3	100 g	30°	1.0
4	400 g	30°	1.0

The choice of cone depends on the penetration depth, as only depths in the interval of 7-20 mm are valid. For the first test (1 h after gelling), cone number 3 was used. The choice of cone for the later tests was determined based on previous penetration depths. Due to the width of the containers, it is possible to fit three drops of cones 1-3 without compromising the results. In cases where more than one drop was performed for a sample, an average of the valid results was used for the calculations.

Figure 5 - Container for the fall cone test samples

Figure 6 – Fall cone test apparatus.

3.2.2. Uniaxial compression test

The uniaxial compression tests were performed in intervals, with the first test being performed 24 hours after gelling and subsequent tests performed every 24 hours after for four days (Tuesday to Friday). In total, 24 samples, three for each accelerator per day, were prepared on the first day of the week. The samples for the uniaxial compression test were stored in room temperature with a small amount of water covering the silica sol in each sample to prevent drying. For this test, the containers are cylindrical plastic tubes with caps on both sides, able to prevent any disturbance of the sample. White Vaseline was coated on the inside of the cylinders to prevent the silica sol from sticking to the inside of the containers. In order to prepare the samples for this test, a 10 liter bucket was used. The bucket was filled with 4125 g (3200 ml) of silica sol for both accelerators, while 767.9 g (714 ml) of NaCl and 435.4 g (400 ml) of KCl was used for the preparation of each solution. Since the bulk amount was too large to effectively stir using magnetic stirring, the samples were stirred manually using a metallic rod. A 10at spring was used for all tests.

1. A sample of silica sol gel is prepared in a cylindrical plastic tube with an inner diameter of 50 mm, as explained above (see figure 7).
2. The sample is removed from the cylinder and cut to size before being placed in the uniaxial compression test apparatus (see figure 8). The spring type is noted (10at was used for all tests).
3. The apparatus is switched on and left to run until failure occurs, at which point it is turned off.
4. A load-deformation graph is plotted on pressure sensitive paper, where the plateau of the curve marks the load weight, m_{load}.

5. The undrained shear strength is determined using the formula $\tau_u = \frac{\sigma}{2}$, where σ is the compressive strength, $\sigma = \frac{m_{load} \cdot g}{A}$, and m_{load} is the load weight (taken from the graph), g is the gravitational acceleration and A is the cross-sectional area of the sample.

Figure 7 – Cylindrical container used to mould and store the silica sol samples for the uniaxial compression test.

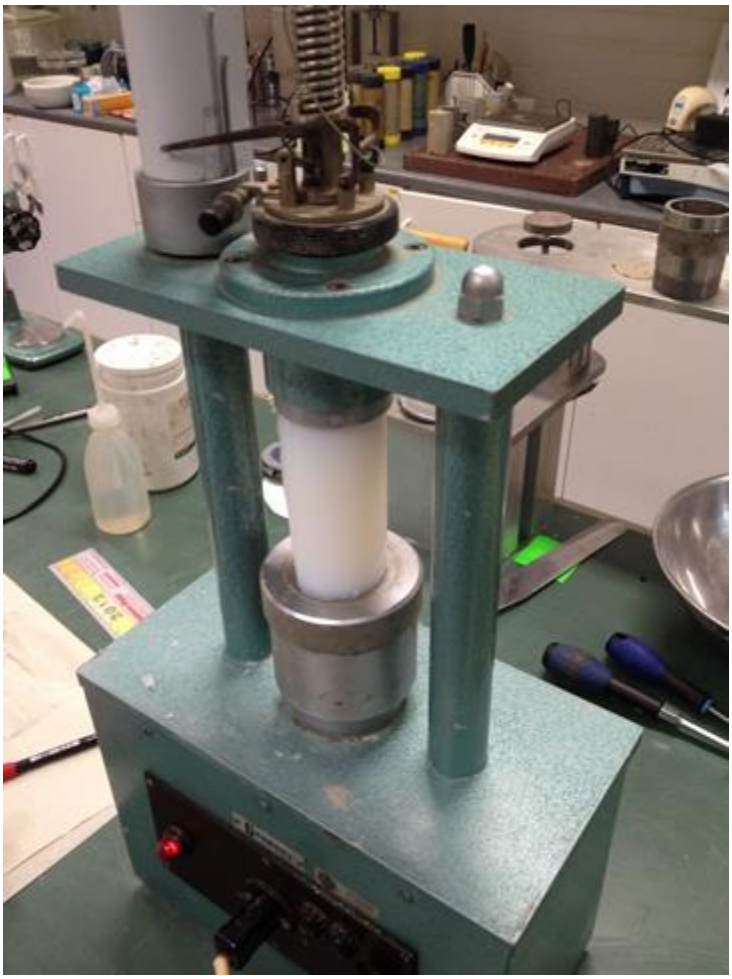

Figure 8 - Compression test apparatus. The spring and the pressure sensitive paper are shown on the top of the machine.

3.3. Rheological tests

This section contains the test procedure for the rheological tests. The aim of these tests is to find the viscosity and shear strength development of the silica sol during the gelling process. To do this, a two types of tests will be performed – a viscometric test using a cup and bob setup, and an oscillating test using an oscillating plate setup. The aim of the cup and bob test is to find the viscosity development of the silica sol over time, while the aim of the oscillating plate test is to find how the shear strength develops as the viscosity increases. Figure 9 shows the rheometer used, with the oscillating plate setup installed.

Figure 9 – Rheometer with oscillating plate setup.

3.3.1. Viscometric test – cup and bob

The viscometric test using the cup and bob setup is performed in two runs with the same parameters. The cup used has an inner diameter of 27.5 mm and the bob is blasted with a diameter of 25 mm. A gap length of 4.000 mm is used. A bulk sample for each salt will be prepared according to table 1 and a small amount of the prepared silica sol from the bulk sample is used in the test. The remaining silica sol in the larger sample will be used for controlling the gel time using the visual method. The temperature of the samples will be controlled by placing them in a 20 °C water bath four hours prior to the test.

1. Fill two containers with 70 ml silica sol, one with 16 ml of 2 M NaCl solution and one with 8 ml of 2 M KCl solutions. All the containers need to be properly sealed so as to not spill into the water bath.
2. Place the containers in a 20 °C water bath for four hours prior to the experiment.
3. Mix one sample of silica sol with one of the accelerators using a magnetic stirrer. Pour the salt solution into the silica sol for 5 seconds and let it stir for 15 seconds.
4. Use a pipette to pull 15 ml of the prepared solution.
5. Place the solution into cup and start the rheometer. Note that time.
6. Note the time of gelling using the visual method.
7. Repeat for the other salt solution.

The data points from this test will be plotted in excel in order to visualize the viscosity development with respect to time.

3.3.2. Oscillating plate test

The oscillating plate test is performed in two runs similar to the viscometric test. The plates in the test setup have a diameter of 40 mm and 60 mm for the upper and lower plate respectively. The upper plate is conical, with a 4° cone angle. A gap length of 0.150 mm between the plates is used. For this test, a 60 second pre-shear with a shear rate of 10 s^{-1} will be used to ensure that the gap is completely filled with the material. The oscillation frequency is set to 1 Hz and the strain to 0.5 %. As was described for the viscometric test, a small amount of the prepared silica sol from the bulk sample is used, with gel times being controlled for the larger sample. The temperature of the samples will be controlled by placing them in a 20 °C water bath four hours prior to the test.

1. Fill two containers with 70 ml silica sol, one with 16 ml of 2 M NaCl solution and one with 8 ml of 2 M KCl solutions. All the containers need to be properly sealed so as to not spill into the water bath.
2. Place the containers in a 20 °C water bath for four hours prior to the experiment.
3. Mix one sample of silica sol with one of the accelerators using a magnetic stirrer. Pour the salt solution into the silica sol for 5 seconds and let it stir for 15 seconds.
4. Take a small amount of liquid and place between the plates. Ensure that the gap between the plates is completely filled with silica sol and wipe away any excess material around the upper plate.
5. Start the test and let it run until gelling.
6. Note the time of gelling using the visual method.
7. Repeat the procedure for the other salt solution.

The data points from this test will be plotted in excel in order to visualize the shear strength development with respect to viscosity.

3.4. Fracture replica

This section contains the theoretical background and test procedure for the fracture replica test. The aim of this test is to investigate if the silica sol is susceptible to erosion due to the shear stress caused by the water. To find the shear stress of the water, the hydraulic gradient and the hydraulic aperture of the fracture replica must be found.

3.4.1. Test setup

The test equipment for this test consists of four parts (see figure 10) – a pressure regulator (A), two tanks (one for silica sol and one for water) (B) and a fracture replica (C).

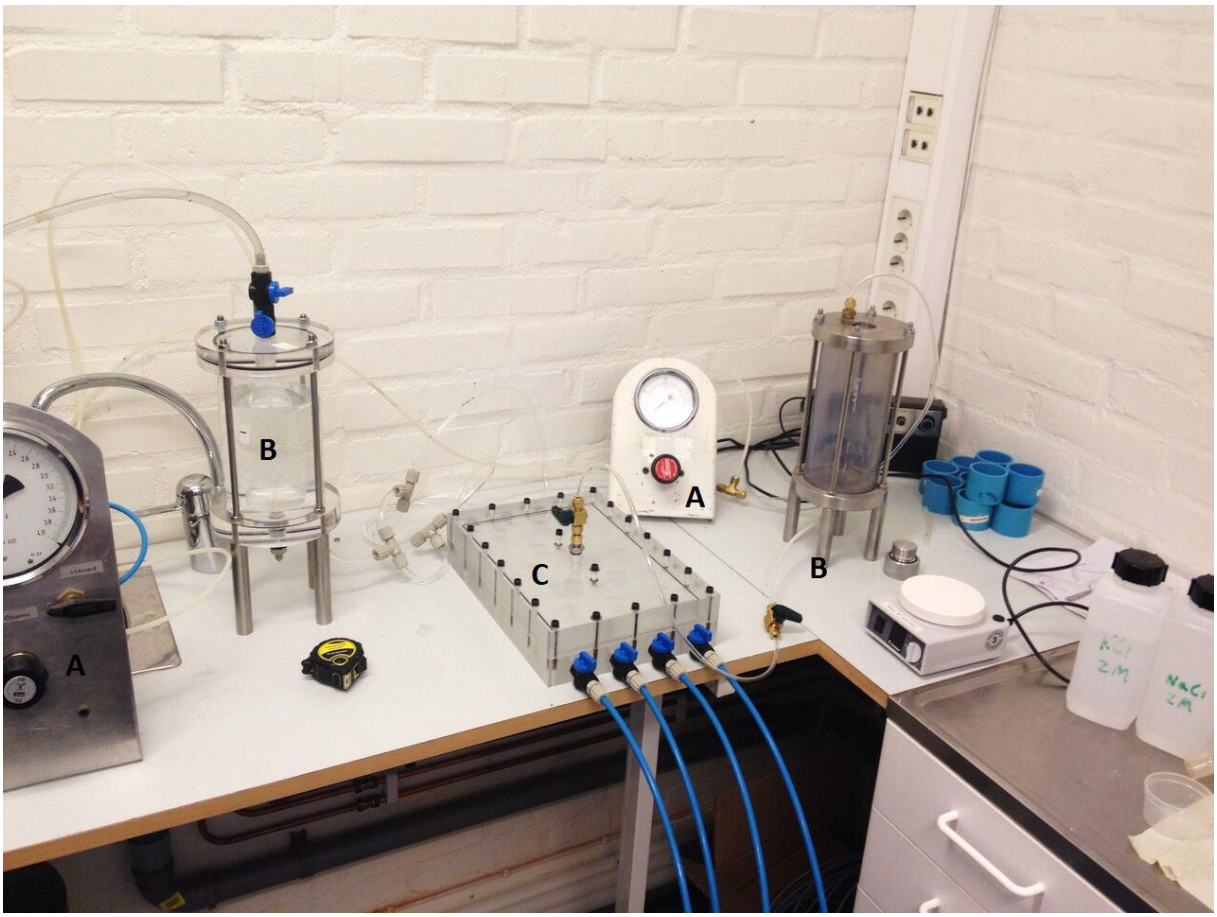

Figure 10 - Fracture replica test set-up.

3.4.2. Determining hydraulic gradient

To determine the hydraulic gradient, the loss of head through the fracture replica must be found. This is done by letting water flow from the tank through the replica and into a tall glass cup. The flow of water will stop when the head of the water is equal to the sum of the losses in the fracture replica and the head of the water in the cup. Therefore, the loss of head can be calculated as

$$\Delta H = h_2 + z_2 - (h_1 + z_1)$$

where h_1 is the head of the water in the tank, z_1 is the height of the tank above the floor, h_2 is the head of the water in the cup and z_2 is the height of the cup above the bench. For this experiment, the tank was placed at a height of 28 cm above the bench and the cup was placed right on the bench, giving it a height of zero. To calculate the hydraulic gradient, the loss of head is divided by the length of the fracture replica. In this experiment, the replica is 30 cm long.

3.4.3. Determining hydraulic aperture

The hydraulic aperture can be calculated using the cubic law (Witherspoon et al., 1980)

$$\frac{Q}{-\Delta H} = 8Cb^3$$

where Q is the flow, ΔH is the loss of head, b is the aperture and C is a constant. Note that ΔH is negative, so the expression gives a positive number. For straight flow through a fracture, C can be calculated as

$$C = \frac{W\rho_w g}{12L\mu_w}$$

where W is the width of the fracture replica, L is the length, ρ_w is the density of water, g is the gravitational constant and μ_w is the viscosity of water. For this experiment, the width of the fracture replica is 20 cm, the length is 30 cm and the flow through the replica is $6.5*10^{-6}$ m^3/s. The density and viscosity of the water were chosen for a temperature of 20 °C.

3.4.4. Shear stress of water

Once the hydraulic gradient and the hydraulic aperture of the fracture replica are known, it is possible to calculate the shear stress of water using the following equation (modified from Axelsson, 2009)

$$\tau_{water} = \frac{\rho_w \cdot g \cdot b}{2} \cdot \left(-\frac{\Delta H}{L}\right)$$

where τ_{water} is the shear stress of the water, ρ_w is the density of water, g is the gravitational constant, b is the hydraulic aperture and $-(\Delta H/L)$ is the hydraulic gradient.

3.4.5. Determining the grouting overpressure

The grouting overpressure can be calculated if the maximum penetration, the gel induction time and the initial viscosity of the silica sol are known. However, an easier method is to simply raise the tank containing the silica until the sought after penetration is achieved. For this test, the second method was chosen due to its simplicity. The required height of the silica sol to achieve a 10 cm penetration length was found to be 38 cm.

3.4.6. Erosion test

The aim of the erosion test is to find if the silica sol will erode due the pressure of the water in the fracture replica. This test will be conducted by letting water flow through the replica and then grouting until gelling (approximately 20 minutes) with the overpressure as described

above. Once gelling occurs, the packer is closed and the replica is observed for 5 minutes to see if any erosion occurs. The erosion test will be conducted for both the accelerators, so that a comparison can be made.

The results from the oscillating plate test will be used in order to determine the shear strength of the silica sol at gelling. If the shear stress exerted by the water, as calculated above, is lower than the shear strength of the silica sol at gelling, the silica sol should not be susceptible to erosion.

The samples of silica sol for this experiment will be prepared in a large bucket and stirred using magnetic stirring. 644 g of silica sol (500 ml) will be used for both samples, with 120 g of NaCl solution and 68 g of the KCl solution, for the NaCl and KCl samples, respectively.

4. RESULTS

4.1. Determining the gel time

The recorded amount of salt solution and the recorded gel times are presented in table 5.

Table 5 – Recorded gel times and salt amounts.

NaCl		KCl	
Added salt (ml)	Gel time (min)	Added salt (ml)	Gel time (min)
5.00	14	5.00	1
4.50	18,5	3.50	4
4.46	20.5	2.50	18.5
4.44	21	2.44	15.5
4.00	22+	2.44	15
3.00	22+	2.30	20.5
n/a	n/a	1.00	22+

As can be seen, the required amount of solution to achieve a 20 minute gel time was 4.46 ml of NaCl solution and 2.30 ml. Table 6 contains unit conversions for convenience. The concentration of the salt solution was 2 M. Also note that the values in the fourth column of table 6 refer to the mass of salt per volume of silica sol, and not the mass of salt solution per volume of silica sol.

Table 6 – Unit conversions.

NaCl	4,46 ml/20 ml Si sol	0.223 ml/ml Si sol	26 mg/ml
KCl	2,30 ml/20 ml Si sol	0.115 ml/ml Si sol	17 mg/ml

Determining the amount of salt solution needed for a gel time of 20 minutes is essential for ensuring that the results of the other tests are comparable. However, even though care has been taken to ensure a constant gel time of 20 minutes for all tests, variation in gel time between 19-23 minutes have generally been observed. This variance is likely due to measuring inaccuracy, as the equipment used to prepare the samples for the determination of the gel time was more accurate than the equipment used to prepare the samples for the other tests. The stirring rate of the samples may also affect the gel time. The variance in gel time may also be due to temperature differences, as the temperature was not actively controlled for most of the tests in this report.

4.2. Mechanical tests

This section contains the results for the fall cone test and the uniaxial compression test. The results are divided by test type (fall cone test and uniaxial compression test).

4.2.1. Fall cone test

Figure 11 shows the results for the fall cone test. As can be seen from the figure, the shear strength for silica sol mixed with NaCl has a lower shear strength than silica sol mixed with KCl. Silica sol mixed with NaCl has a shear strength that increases from 3 kPa one hour after gelling to 20 kPa five days after gelling. Silica sol mixed with KCl has a shear strength that increases from 5 kPa one hour after gelling to 23 kPa five days after gelling.

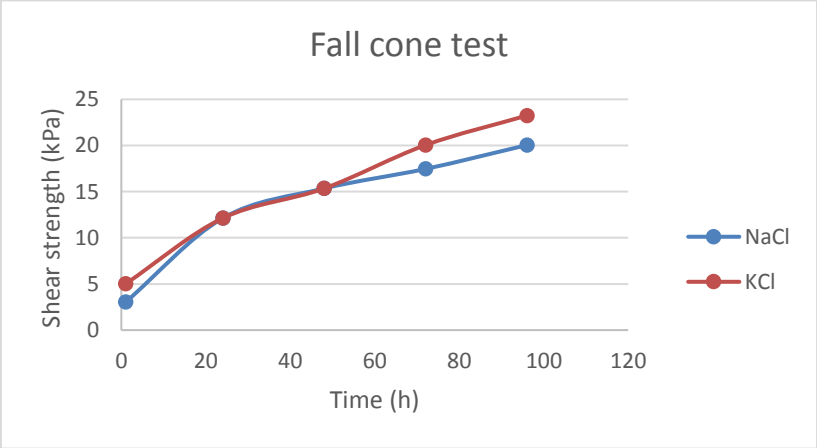

Figure 11 – Results for the fall cone test.

4.2.2. Uniaxial compression test

Figure 12 shows the results for the two accelerators. Both curves have a similar appearance, and the shear strength of NaCl increases from 7 kPa to 15 kPa over time while the shear strength of KCl is consistently higher, with a shear strength increasing from 11 kPa to 18 kPa over time. As was the case for the fall cone test, KCl gives a higher shear strength than NaCl. However, the shear strength found from the uniaxial compression test is lower than shear strength found from the fall cone test. This difference may be due to the samples being damaged while cut into size for the test apparatus, causing the cross-sectional area to be smaller than what has been used in the calculations. This would lead to an underestimation of the shear strength. It may also be due to using mechanical stirring instead of magnetic stirring, which is much less effective and may have impacted the strength development.

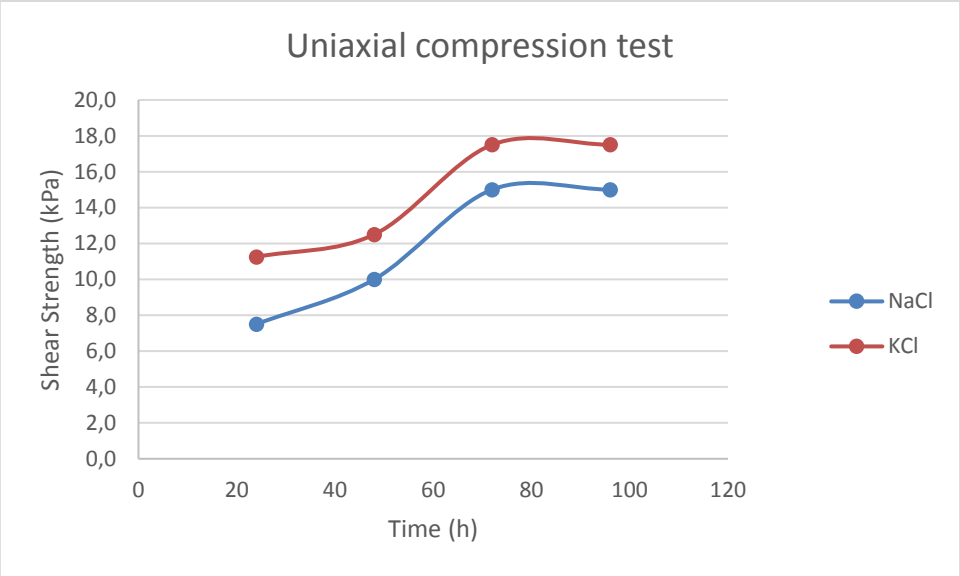

Figure 12 – Results for the uniaxial compression test.

An interesting observation during the uniaxial compression test is the vertical failure plane exhibited by some of the tested samples, see figure 13. This behaviour is consistent with results from Butrón, Axelsson and Gustafson (2007). Nonetheless, there is reason to be sceptical of this observation. As shown by Axelsson (2006), silica sol is a ductile material at gelling that becomes more brittle as strength increases. However, ductile material would produce a cone-shaped fracture, while a brittle material produces a fracture plane at a 45° angle to the specimen axis (Norton, 2013). Thus, the vertical fracture plane is to be considered an anomalous behaviour and the samples that produced this behaviour were considered invalid for this test. In fact, this anomalous behaviour was so prevalent in the tested samples that only a single valid result for each accelerator was recorded for each day of testing, severely impacting the amount of data that could be gathered from the uniaxial compression test.

The occurrence of the vertical fracture plane may be due to the test apparatus – it was observed during the testing of the samples that there is a strong cohesion between the samples and the testing apparatus. This cohesion may cause tensile stresses in the samples that may account for the vertical fracture plane displayed during testing. If this is the case, it follows that the uniaxial compression test may be unsuitable for the testing of silica sol. However, it should be noted that during a complementary test performed by Johan and Emilia Funehag in the final stage of this project, thin plastic membrane was placed between the samples and the apparatus, see figure 14. As can be seen from figure 14, the specimen did not produce a vertical fracture during testing. This may indicate that the strong cohesion between the samples and the testing apparatus is the main reason for the vertical fractures. However, more tests have to be performed in order to fully understand this behaviour.

Figure 13 – Vertical fracture plane consistent with the results of Butrón, Axelsson and Gustafson (2007).

Figure 14 – Cone-shaped fracture of the specimen after using membranes during a uniaxial compression test (Photo taken by Emilia Funehag).

4.3. Rheological tests

This section contains the results of the viscometric test and the oscillating plate test. The results are divided by test type.

4.3.1. Viscometric test – cup and bob

Figure 15 shows the viscosity development of silica sol mixed with NaCl and KCl (see appendix 1 for raw data). Both accelerators give an exponential increase in viscosity over time when plotted in a log-lin diagram. This is to be expected, given the very rapid viscosity increase that can be observed for silica sol in general.

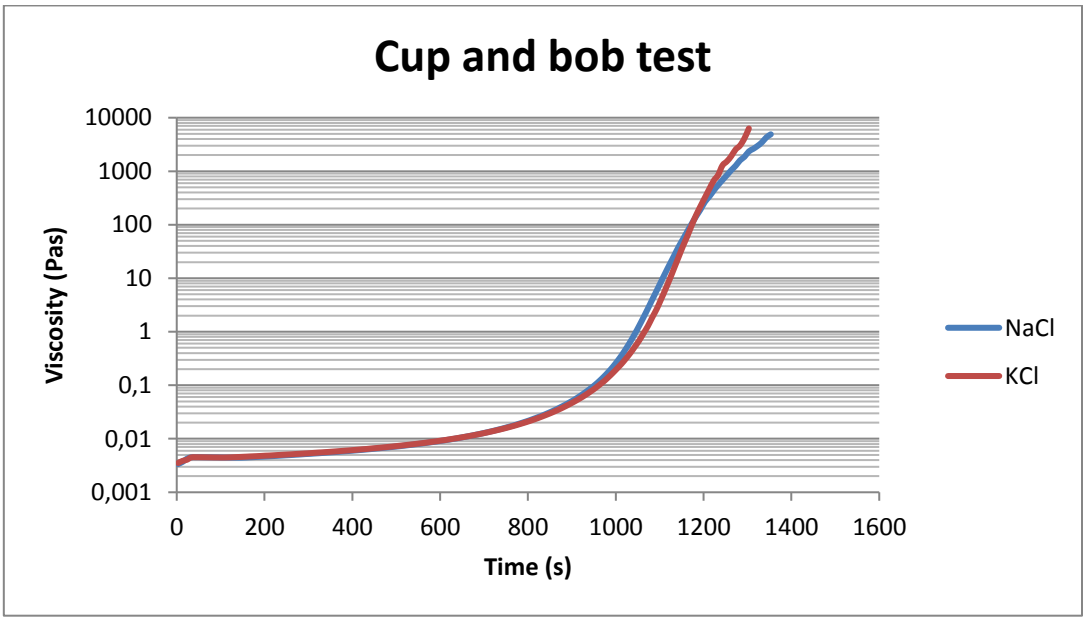

Figure 15 – Viscosity development of silica sol over time

As can be seen in figure 15, the viscosity development is almost identical for both accelerators. This is to be expected for two samples of silica sol with the roughly the same gel time. Some slight discrepancies can be seen, likely due to a difference in gel time (controlled using the visual method) for the two samples – 20 minutes for the sample mixed with NaCl and 22 minutes for the sample mixed with KCl. The viscosity starts to increase rapidly at around 400-500 seconds for both accelerators. These results suggest that the difference in strength between the two accelerators that was observed during the mechanical testing occurs primarily after gelling. It is also worth noting that the rapid increase in viscosity occurs after roughly half the gel time, consistent with the description of the gel induction time by Funehag (2007).

4.3.2. Oscillating plates

Figures 16 shows the shear strength development of the silica sol with respect to viscosity for NaCl and KCl (see appendix 2 and 3 for raw data). As can be seen, the shear strength increases exponentially with increased viscosity. The shear strength of the silica at gelling was found to be 59 Pa for the NaCl sample and 82 Pa for the KCl sample. These findings confirm the results from Axelsson (2009), where the shear strength of silica sol at gelling was predicted to be in the range of 60-80 Pa.

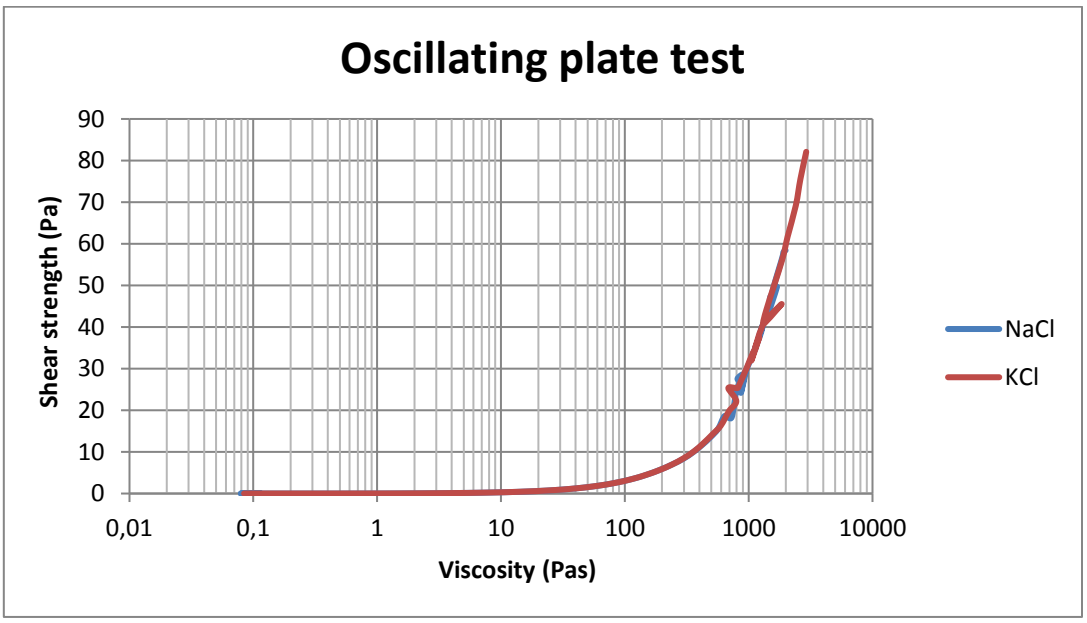

Figure 16 – Shear strength development of silica sol with respect to viscosity

As can be seen in figure 16, the shear strength development is almost identical for both accelerators. While the shear strength is higher for silica sol mixed with KCl than for silica sol mixed with NaCl, a result that has been consistent for all tests in this project, this is likely due to the difference in gel time for the two samples. The gel time for the sample of silica sol mixed with NaCl was found to be 22 minutes using the visual method. For the sample mixed with KCl, the gel time was found to be 19 minutes using the visual method. Since the gel time is shorter for the sample mixed with KCl, it is expected that the shear strength would be higher for this sample. Since both the viscosity and shear strength development during the gelling process is identical for both accelerators, it seems reasonable to assume that the difference in shear strength observed in the other tests occur after gelling.

It is also interesting to note that there seems to be two disturbances in the shear strength-viscosity plot. These disturbances persist between both accelerators and occur at around 800 Pas and 1500 Pas. The disturbances are likely a result of methodology – as the silica sol gels it seems as if slipping occurs between the silica sol and the surface of the plates. This could possibly be remedied by trying different test setups – something similar to a cup and bob setup may work better, for instance.

4.4. Fracture replica

This section contains the results for the fracture replica test, namely the determined hydraulic gradient, hydraulic aperture and shear stress of water as well as the results of the erosion test.

4.4.1. Hydraulic gradient, hydraulic aperture and shear stress of water

Table 7 shows the measurements done to find the hydraulic gradient and figure 17 shows an illustration of the measurements for ease of understanding. The pressure head of the water in the tank was found to be 14.3 cm when the flow stopped and the pressure head in the measuring cup was found to be 10 cm. This gives a hydraulic gradient of -0,923, according to the equation in chapter 3.4.2.

Table 7 – Measurements for the calculation of the hydraulic gradient.

z_1	28 cm
h_1	14.3 cm
z_2	0 cm
h_2	10 cm
ΔH	-32.3 cm
$\Delta H/L$	-1.077

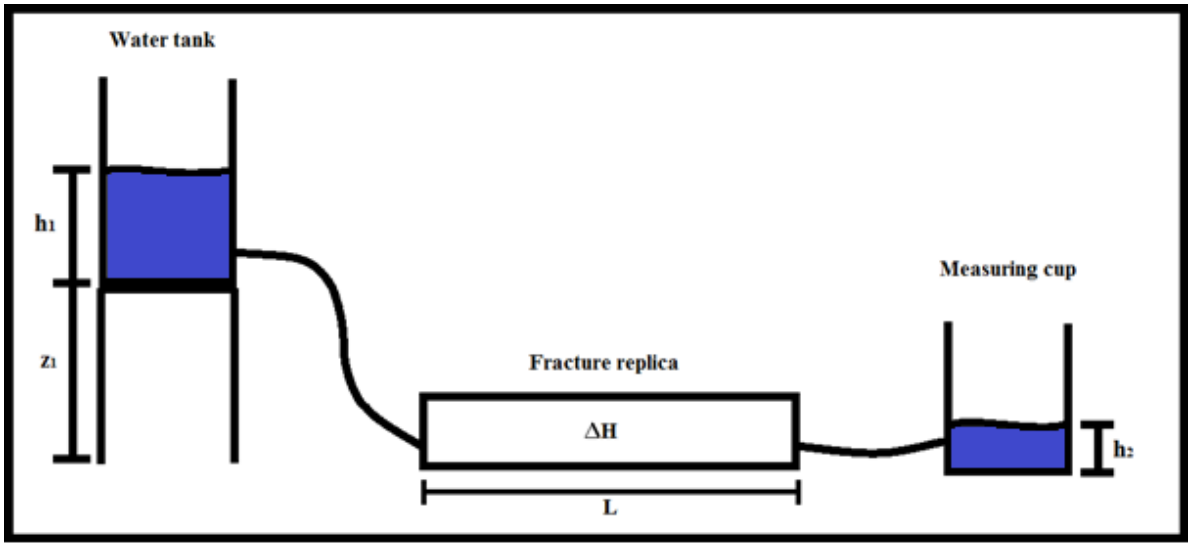

Figure 17 – Illustration of the measurements found in table 7.

The hydraulic aperture was calculated to be 167.2 µm at 20 °C, using the equations in chapter 3.4.3.

Given the above mentioned hydraulic gradient and hydraulic aperture, the shear stress of water was calculated to be 0.883 Pa, according to the equation in chapter 3.4.4.

4.4.2. Erosion test

Figures 18 and 19 show the grout in the fracture replica 5 minutes after gelling – the first picture showing the NaCl grout and the second showing the KCl grout. As can be seen in the figures, no visible erosion has occurred for either of the accelerators. These results suggest that both accelerators give a grout that is capable of withstanding the shear stress of the water in this grouting scenario.

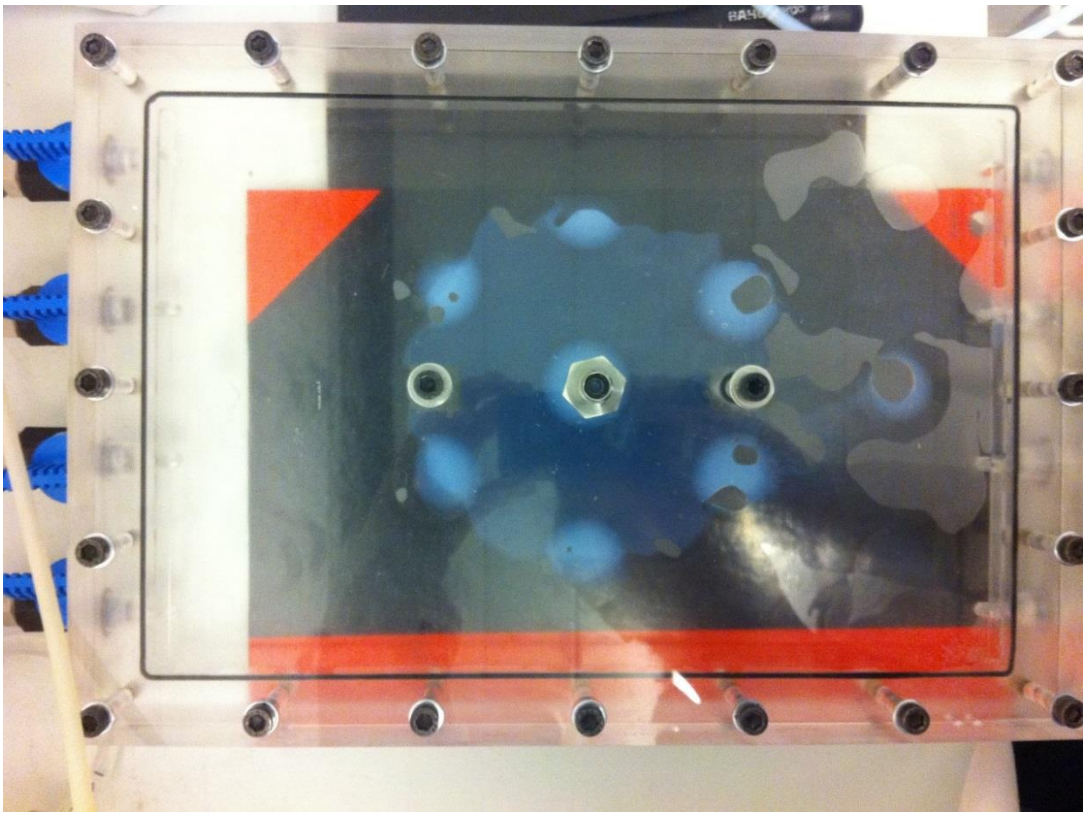

Figure 18 – NaCl grout at 5 minutes after gelling.

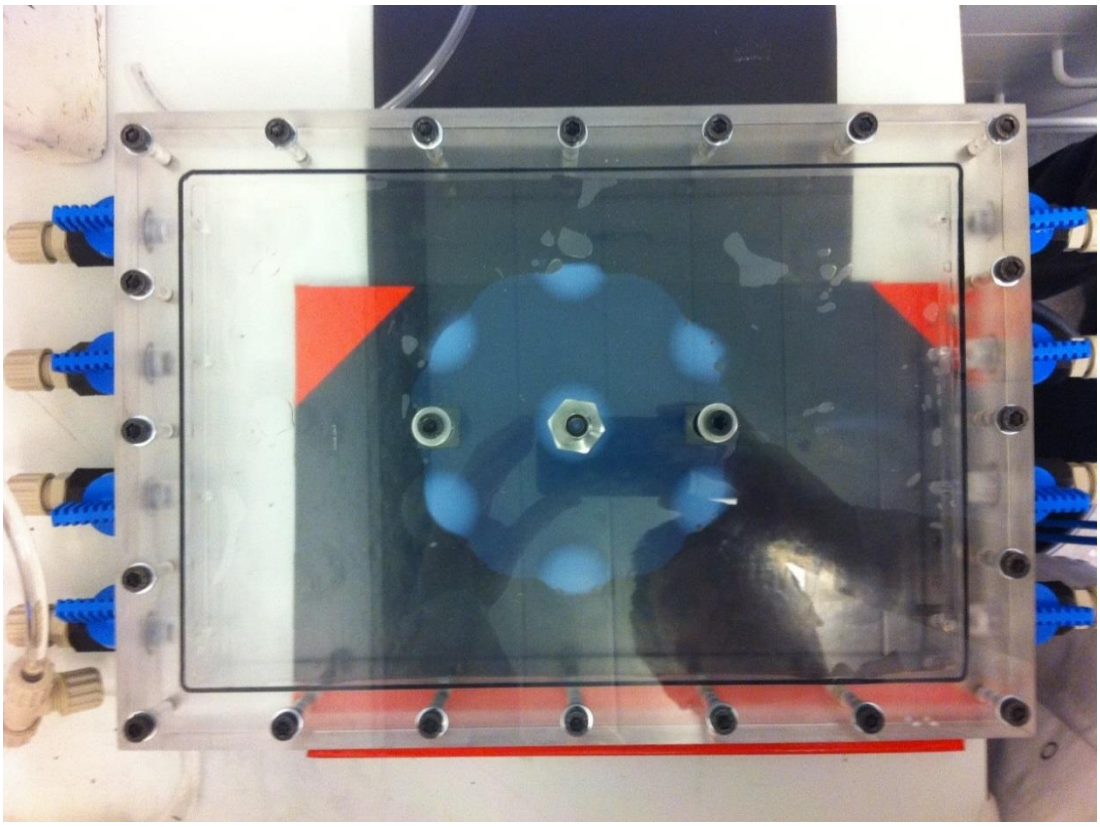

Figure 19 – KCl grout at 5 minutes after gelling.

It should also be noted that the method of controlling the grouting overpressure (raising the silica sol tank) is less than optimal. Even though pressure regulators were a part of the test setup for the fracture replica, they were not accurate enough. Attempts at regulating the pressure using pressurized air were not successful due to this limitation, as the overpressure was frequently much too high when the regulators were used. Further studies on the erosion of silica sol, using more accurate equipment, would be necessary to ensure that the results of this study are reliable.

5. DISCUSSION

One of the objectives of this project has been to determine the shear strength development of silica sol, both at gelling and over a period of five days. To complete this objective, three different tests have been performed – the fall cone, uniaxial compression and oscillating plate tests. In order to fully understand the results, it is necessary to discuss if these tests measure the right parameters and if the results from the different tests are comparable. To this end, it is worth noting the differences between the results from the fall cone and uniaxial compression tests. The shear strength, as calculated for the fall cone test, is consistently higher than the shear strength calculated for the uniaxial compression test. While this difference may be due to errors in sample preparation, it may also be due to the uniaxial compression test being unsuitable for measuring the shear strength of silica sol. The latter possibility arises due to the observation that the fracture planes of the samples in the uniaxial compression test are consistently vertical. A brittle material like hardened silica sol should display a fracture plane at a 45° angle. This difference in behavior may indicate that the uniaxial compression test does not properly measure the shear strength of silica sol. If this is the case, then the fall cone test and the uniaxial compression test cannot be compared.

The results from the oscillating plate test cannot be directly compared to the results from the fall cone test, as these tests are performed in different time frames. However, due to the observed exponential increase in shear strength with viscosity, it is not unreasonable to assume that the shear strength of the silica sol would be able to rise from 60-80 Pa at gelling to 3-5 kPa after one hour. Furthermore, a shear strength at gelling of 60-80 Pa is consistent with the prediction made by Axelsson (2009), which was based on fall cone test data. Therefore, it is likely that both the fall cone test and the oscillating plate test properly measure the shear strength of silica sol.

Another objective of this thesis was to investigate possible differences between the two accelerators – NaCl and KCl. This has been done by investigating the shear strength and the viscosity of silica sol mixed with NaCl or KCl. The results show that KCl gives a consistently higher shear strength than NaCl, for all tests. It has also been found that the viscosity development over time and the shear strength development with respect to viscosity are identical for both accelerators. This result suggests that the difference in shear strength between the two accelerators starts to develop after gelling.

Determining the erosion stability has been yet another objective of this project. This has been done by grouting a fracture replica and observing if any noticeable erosion occurs. As stated, no erosion could be seen in the studied scenario. It is, however, important to link the erosion susceptibility of the silica sol to its shear strength. While the grout in this scenario is able to resist the erosion due to water stress, it is important to note that a water stress of less than 1 Pa is very low. This can be compared with the calculated water stress from Reynisson (2014), where the average water stress was in the range of 5-13 Pa, depending on calculation method. However, it can be safely assumed that the silica sol can withstand water stress much higher than 1 Pa. In Reynisson (2014), the maximum calculated shear stress due to water was in the range of 37-66 Pa, depending on calculation method. Furthermore, Suresh & Tohow (2013)

calculated the shear stress due to water in a service tunnel in Gothenburg and found it to be 25 Pa. If the silica sol has a shear strength at gelling in the range of 60-80 Pa, as suggested by the predictions in Axelsson (2009) and by the findings of the oscillating plate test (as described earlier in this thesis), the silica sol should be able to resist erosion for most common grouting scenarios. This assumption is further justified by a simple observation made during the cleaning of the fracture replica following completion of the erosion test. While cleaning, pressurized water was run through the fracture replica and break down of the silica sol was seen first at a pressure of 20 kPa and 40 kPa for NaCl and KCl, respectively. This suggests that the silica sol possesses a low susceptibility to erosion in most common grouting applications. Therefore, it can be said that the shear strength as found by the oscillating plate test can serve as an indicator of the erosion susceptibility of the silica sol.

6. CONCULUSION

The aim of this project is to investigate the shear strength development and erosion susceptibility of silica sol in grouting applications. In order to do this, three types of tests have been performed – mechanical tests for determining the shear strength after a week; rheological tests, in order to determine the short-term viscosity and shear strength development as well as finding the relationship between shear strength and viscosity; and an erosion test using a fracture replica, in order to determine if the silica sol is at risk of erosion from the stress caused by the water in a fracture. Two types of accelerators – NaCl and KCl – have been used for all the tests and comparisons between the accelerators have been made. From these tests the following conclusions can be drawn:

- Less KCl than NaCl is needed to give a gel time of 20 minutes. This indicates that KCl causes more silica particles to aggregate than NaCl does.
- The shear strength from the uniaxial compression test is generally lower than the shear strength from the fall cone test. This may be due to errors in sample preparation. However, the failure plane of the silica sol in the uniaxial compression test is almost completely vertical, a result that is consistent with Butrón, Axelsson and Gustafsson (2007). Since silica sol is a ductile material at gelling that becomes more brittle with time, it should first display a cone-like fracture that gives way to a 45° failure plane as the silica sol hardens and becomes more brittle. This may indicate that the uniaxial compression test cannot test the shear strength of silica sol properly. However, adding membrane sheets between the specimen and the apparatus seem to remedy this.
- The viscosity increases exponentially over time, with a rapid increase in viscosity occurring after almost half the gel time.
- In a lin-log plot, the shear strength of the silica sol increases exponentially with viscosity.
- Silica sol mixed with NaCl has a slightly lower shear strength than silica sol mixed with KCl. The shear strength development as a function of viscosity and the viscosity development are identical for both accelerators. This indicates that any difference in shear strength between NaCl and KCl occurs after gelling. However, since the difference in shear strength between the accelerators is small, it cannot be said with certainty that this difference is not due to a systematic error during testing.
- No erosion can be seen for silica sol mixed with either accelerator under the conditions that have been studied in this project.
- While the water stresses that have been used in this thesis are low (less than 1 Pa), a case can be made that silica sol is capable of withstanding much higher stress. A shear strength of 60-80 Pa at gelling, consistent with predictions from Axelsson (2009), is enough to withstand the conditions in both Suresh & Tohow (2014) and Reynisson (2014). It can be concluded that silica sol should be able to withstand erosion due to water stress in most common grouting applications.

6.1. Further investigations

In order to fully understand the properties of silica sol more research is necessary. It would be especially interesting to perform more in-depth rheological tests of the material, such as investigating the Winter-Chambon criteria. Since the choice of accelerator seems to have an impact on the shear strength of the silica sol, it would be worthwhile to test the properties of silica sol mixed with different accelerators. Further studies on the erosion resistance of silica sol using a fracture replica and more exact equipment for pressure regulation would also be necessary in order to fully understand the relationship between erosion susceptibility and shear strength. Finally, investigating the effect of different grouting environments on the erosion susceptibility of silica sol would yield a deeper understanding of how to properly use the material in grouting applications.

REFERENCES

Axelsson, M. (2006). Mechanical tests on a new non-cementitious grout, silica sol: A laboratory study of the material characteristics. *Tunnelling and Underground Space Technology*, 21, pp. 554-560.

Axelsson, M. (2009). *Prevention of erosion in fresh grout in hard rock*. Göteborg: Chalmers University of Technology.

Bohlin Instruments, 1994. A basic introduction to rheology. [Online] Available at: http://www.iesmat.com/iesmat/upload/file/Malvern/Productos-MAL/REO-A%20basic%20introduction%20to%20rheology.pdf
[Accessed May 2016].

Butrón, C. (2005). *Mechanical behaviour of silica sol*. Göteborg: Chalmers University of technology.

Butrón, C., Axelsson, M. and Gustafson, G. (2007). *Silica Sol for Rock Grouting – Tests on Mechanical Properties*. Göteborg: Chalmers University of Technology.

Butrón, C., Axelsson, M. and Gustafson, G. (2009). Silica sol for rock grouting: Laboratory testing of strength, fracture behaviour and hydraulic conductivity. *Tunnelling and Underground Space Technology*, 24, pp. 603-607.

Funehag, J. (2007). *Grouting of fractured rock with silica sol; Grouting design based on penetration length*. Göteborg: Chalmers University of Technology.

Funehag, J. and Gustafson, G. (2008). Design of grouting with silica sol in hard rock – New methods for calculation of penetration length, Part I. *Tunnelling and Underground Space Technology*, 23, pp. 1-8.

G.I.T. Laboratory Journal 3-4/2007, pp 68-70, GIT VERLAG GmbH & Co. KG, Darmstadt. [Online]
Available at: http://www.mate.tue.nl/~wyss/files/Wyss_GIT_Lab_J_2007.pdf
[Accessed January 2016].

Hansbo, S. (1957). *A new approach to the determination of the shear strength of clay by the fall cone test*. Swedish Geotechnical Institute, Stockholm.

Kyoto Electronics Manufacturing, 2014. Classical Rotational Viscometers (Rheometers). [Online] Available at: http://www.ems-viscometer.com/
[Accessed May 2016].

Malvern, n.d., Rheometers for measuring viscosity and viscoelasticity - from formulation to product use. [Online] Available at: http://www.malvern.com/en/products/measurement-type/rheology-viscosity/default.aspx
[Accessed January 2016].

Norton, R. L. (2013). *Machine Design – an integrated approach.* 5:th edition, London: Pearson.

Persoff, P., Apps, J. A., Moridis, G. J. and Whang, J. M. (1997). Effect of Dilution and Contaminants on Strength and Hydraulic Conductivity of Sand Grouted with Colloidal Silica Gel. In: *1997 International Containment Technology Conference and Exhibition*. St. Petersburg, FL: Ernest Orlando Lawrence Berkeley National Laboratory.

Persoff, P., Moridis, G. J., Apps, J. A. and Pruess, K. (1998). Evaluation Tests for Colloidal Silica for Use in Grouting Applications. *Geotechnical Testing Journal*, 21, pp. 264-269.

Schramm G., "A practical approach to Rheology and Rheometry", 2nd Edition 2004, Thermo Electron Karlsruhe.

Suresh, K. and Tohow, M. (2013). *Grouting of a difficult borehole*. Göteborg: Chalmers University of Technology.

TA Instruments, n.d., ARES-G2 rheometer manual. [Online] Available at: http://www.tainstruments.com/pdf/brochure/BROCH-ARESG2-2014-EN.pdf [Accessed January 2016].

Winter, H. H. and Chambon, F. (1986). Analysis of Linear Viscoelasticity of a Crosslinking Polymer at the Gel Point. *Journal of Rheology*, 30, pp. 367-384.

Witherspoon, P. A., Wang, J. S. Y., Iwai, K., Gale, J. E. (1980). Validity of Cubic Law for Fluid Flow in a Deformable Rock Fracture. *Water Resources Research,* 16(6), pp. 1016-1024.

Ågren, P. and Rosenholm, J. B. (1998). Phase Behavior and Structrual Changes in Tetraethylorthosilicate-Derived Gels in the Presence of Polyethylene Glycol, Studied by Rheological Techniques and Visual Observation. *Journal of Colloid and Interface Science,* 204, pp. 45-52.

Reynisson, R. Ö. (2014). *Erosion of Silica Sol in Post Grouted Tunnel at Great Depth.* Göteborg: Chalmers University of Technology.

Appendix 1 – Cup and bob test raw data

NaCl		KCl	
Time '(s)	Viscosity '(Pas)	Time '(s)	Viscosity '(Pas)
3,026	3,37E-03	3,027	3,52E-03
13,026	3,69E-03	13,025	3,86E-03
23,027	4,23E-03	23,026	4,05E-03
32,187	4,49E-03	32,18	4,47E-03
42,386	4,53E-03	42,383	4,52E-03
52,29	4,53E-03	52,282	4,51E-03
62,183	4,51E-03	62,179	4,51E-03
72,385	4,51E-03	72,383	4,49E-03
82,289	4,50E-03	82,284	4,48E-03
92,184	4,48E-03	92,177	4,47E-03
102,382	4,47E-03	102,379	4,47E-03
113,025	4,46E-03	112,281	4,48E-03
122,182	4,45E-03	122,173	4,50E-03
132,379	4,44E-03	132,376	4,54E-03
142,283	4,43E-03	142,276	4,57E-03
152,177	4,45E-03	152,175	4,61E-03
162,384	4,49E-03	162,371	4,65E-03
172,576	4,53E-03	172,274	4,70E-03
183,025	4,58E-03	182,17	4,74E-03
192,376	4,63E-03	192,372	4,78E-03
202,28	4,67E-03	202,275	4,84E-03
212,176	4,72E-03	212,169	4,87E-03
222,374	4,76E-03	222,368	4,93E-03
232,277	4,81E-03	232,271	4,98E-03
242,172	4,87E-03	242,166	5,03E-03
252,371	4,93E-03	253,031	5,09E-03
262,275	4,98E-03	262,268	5,14E-03
272,171	5,04E-03	272,164	5,20E-03
282,369	5,10E-03	282,366	5,26E-03
292,274	5,18E-03	292,268	5,32E-03
302,168	5,22E-03	303,068	5,38E-03
312,37	5,30E-03	312,364	5,45E-03
322,272	5,36E-03	322,263	5,52E-03
332,166	5,44E-03	332,16	5,58E-03
342,365	5,51E-03	342,359	5,66E-03
352,269	5,58E-03	352,261	5,74E-03
362,163	5,66E-03	362,158	5,81E-03
372,364	5,75E-03	372,358	5,89E-03
382,265	5,84E-03	382,26	5,98E-03
392,16	5,92E-03	392,155	6,06E-03
402,36	6,01E-03	402,356	6,16E-03
412,265	6,11E-03	412,258	6,26E-03
422,16	6,21E-03	422,153	6,36E-03
432,357	6,32E-03	432,358	6,45E-03
442,262	6,42E-03	442,255	6,57E-03

452,156	6,54E-03	452,151	6,68E-03
462,357	6,66E-03	462,357	6,80E-03
472,261	6,79E-03	472,255	6,92E-03
482,458	6,92E-03	482,15	7,05E-03
492,354	7,05E-03	492,352	7,19E-03
502,257	7,19E-03	502,252	7,33E-03
513,058	7,36E-03	512,449	7,49E-03
522,352	7,50E-03	522,347	7,64E-03
532,255	7,67E-03	532,251	7,81E-03
542,151	7,85E-03	542,449	7,98E-03
553,029	8,06E-03	552,345	8,17E-03
562,252	8,24E-03	563,028	8,37E-03
572,147	8,45E-03	572,444	8,57E-03
582,35	8,68E-03	582,343	8,78E-03
592,251	8,90E-03	592,246	9,01E-03
602,148	9,15E-03	603,071	9,27E-03
612,347	9,43E-03	612,34	9,51E-03
622,249	9,71E-03	622,244	9,79E-03
632,446	1,00E-02	632,444	1,01E-02
642,343	1,04E-02	643,025	1,04E-02
652,248	1,07E-02	652,24	1,07E-02
662,445	1,11E-02	663,067	1,11E-02
672,341	1,15E-02	672,337	1,15E-02
682,244	1,20E-02	682,241	1,19E-02
692,443	1,24E-02	692,44	1,24E-02
702,341	1,30E-02	702,335	1,29E-02
712,245	1,35E-02	712,238	1,34E-02
722,442	1,42E-02	722,436	1,40E-02
732,339	1,48E-02	732,332	1,46E-02
742,24	1,56E-02	742,234	1,53E-02
752,445	1,64E-02	752,434	1,61E-02
762,638	1,73E-02	762,329	1,69E-02
772,534	1,83E-02	772,531	1,79E-02
782,435	1,94E-02	782,43	1,89E-02
792,935	2,07E-02	792,636	2,01E-02
802,838	2,21E-02	802,831	2,14E-02
812,734	2,36E-02	812,728	2,28E-02
822,932	2,54E-02	822,928	2,44E-02
833,023	2,73E-02	832,829	2,62E-02
843,033	2,96E-02	843,029	2,83E-02
853,024	3,21E-02	853,022	3,05E-02
863,023	3,51E-02	863,023	3,31E-02
873,059	3,85E-02	873,052	3,61E-02
883,024	4,24E-02	883,023	3,96E-02
893,025	4,70E-02	893,022	4,36E-02
903,055	5,24E-02	903,05	4,82E-02
913,023	5,89E-02	913,024	5,36E-02
923,024	6,68E-02	923,024	5,99E-02
933,055	7,64E-02	933,048	6,76E-02
943,022	8,81E-02	943,023	7,69E-02
953,024	1,02E-01	953,024	8,80E-02
963,053	1,21E-01	963,045	1,02E-01

973,023	1,45E-01	973,024	1,19E-01
983,024	1,77E-01	983,024	1,41E-01
993,049	2,20E-01	993,044	1,69E-01
1003,023	2,79E-01	1003,023	2,06E-01
1013,023	3,60E-01	1013,025	2,51E-01
1023,049	4,81E-01	1023,042	3,15E-01
1033,024	6,51E-01	1033,025	3,98E-01
1043,025	9,03E-01	1043,024	5,19E-01
1053,046	1,28E+00	1053,039	6,82E-01
1063,024	1,85E+00	1063,023	9,30E-01
1073,024	2,71E+00	1073,022	1,28E+00
1083,043	3,99E+00	1083,036	1,86E+00
1093,023	5,85E+00	1093,025	2,64E+00
1103,024	8,64E+00	1103,024	4,03E+00
1113,04	1,27E+01	1113,035	6,18E+00
1123,024	1,85E+01	1123,023	9,70E+00
1133,023	2,66E+01	1133,022	1,55E+01
1143,038	3,86E+01	1143,035	2,49E+01
1153,023	5,39E+01	1153,024	4,00E+01
1163,023	7,54E+01	1163,023	6,14E+01
1173,036	1,05E+02	1173,031	9,81E+01
1183,022	1,44E+02	1183,023	1,52E+02
1193,024	1,93E+02	1193,023	2,23E+02
1203,035	2,68E+02	1203,031	3,23E+02
1213,023	3,36E+02	1213,023	4,67E+02
1223,023	4,35E+02	1223,024	6,66E+02
1233,032	5,52E+02	1233,03	8,52E+02
1243,023	6,84E+02	1243,023	1,29E+03
1253,023	8,45E+02	1253,022	1,53E+03
1263,03	1,05E+03	1263,029	1,92E+03
1273,023	1,27E+03	1273,022	2,56E+03
1283,023	1,60E+03	1283,022	3,02E+03
1293,03	1,86E+03	1293,025	4,11E+03
1303,022	2,34E+03	1303,024	6,29E+03
1313,022	2,62E+03	n/a	n/a
1323,031	2,98E+03	n/a	n/a
1333,022	3,48E+03	n/a	n/a
1343,023	4,30E+03	n/a	n/a
1353,028	4,89E+03	n/a	n/a

Appendix 2 – Oscillating plate test raw data, NaCl

Time s	Shear Stress Pa	Viscous Modulus Pa	Elastic Modulus Pa	Viscosity Pas
6.046	0.01774	0.6098	0.3923	0.1154
27.24	0.01331	0.264	0.445	0.08235
48.42	0.00241	0.2843	3.484	0.5563
69.59	0.04968	2.481	12.71	2.061
90.77	0.1324	4.356	29.21	4.7
112	0.2902	6.362	60.6	9.698
133.1	0.539	12.2	110.8	17.74
154.3	0.9078	19.97	184.3	29.5
175.5	1.395	29.2	282.1	45.13
196.7	2.011	40.32	408.7	65.37
217.9	2.784	54	567	90.65
239.1	3.675	71.7	757.6	121.1
260.2	4.719	93.37	980.3	156.7
281.5	5.886	113.4	1246	199.1
302.6	7.118	134.8	1542	246.4
323.8	8.406	161.5	1871	299
345	9.943	177.4	2236	357
366.2	11.61	216.1	2622	418.7
387.4	13.49	232	3075	490.8
408.5	15.56	280.6	3551	566.9
429.7	18.65	300.8	4016	641
450.9	18.26	367.2	4558	727.8
472.1	24.92	381	4991	796.7
493.3	26.26	655	5230	838.9
514.5	26.56	717.7	5462	876.7
535.6	27.58	868	5032	812.7
556.8	28.51	685.1	5718	916.6
578	24.18	433.5	5426	866.3
599.2	29.67	578.1	5979	956
620.3	28.9	735.8	5856	939.4
641.5	28.22	563.3	5657	904.7
662.7	29.62	619.3	5960	953.7
683.9	34.25	763.4	6923	1108
705.1	36.66	753.9	7434	1189
726.3	38.64	721.5	7870	1258
747.4	40.51	804.9	8128	1300
768.6	34.43	1040	6961	1120
789.8	38.21	1060	7648	1229
811	41.6	1164	8391	1348
832.2	44.63	941.4	9244	1479
853.4	47.13	650.9	9348	1491
874.6	48.79	1039	1.018E4	1628
895.8	49.77	1036	1.025E4	1639
916.9	49.62	1346	1.055E4	1692
938.1	41.79	1364	8590	1384
959.3	46.09	1508	9231	1489

980.5	49.61	1416	9895	1591
1002	52.75	1532	1.061E4	1706
1023	55.34	612	1.137E4	1812
1044	57.37	1434	1.182E4	1895
1065	58.05	1475	1.192E4	1911
1086	58.43	1600	1.238E4	1987

Appendix 3 – Oscillating plate test raw data, KCl

Time s	Shear Stress Pa	Viscous Modulus Pa	Elastic Modulus Pa	Viscosity Pas
6.046	0.01348	0.3335	0.4107	0.0842
27.25	0.004454	0.5442	2.388	0.3898
48.48	0.0299	0.9847	9.011	1.443
69.71	0.09693	2.525	22.32	3.576
90.94	0.2273	4.661	48.28	7.72
112.2	0.4384	8.559	90.74	14.51
133.4	0.7564	14.22	154.2	24.65
154.6	1.205	22.28	245.5	39.23
175.9	1.799	32.36	365.1	58.33
197.1	2.529	43.25	517	82.56
218.3	3.429	59.1	704.3	112.5
239.6	4.462	74.05	924.9	147.7
260.7	5.624	95.48	1189	189.8
282	6.938	115.3	1500	239.4
303.2	8.398	140	1851	295.4
324.4	10.11	173.6	2260	360.8
345.6	12.02	195.2	2686	428.7
366.8	14.2	221.4	3192	509.2
388	16.31	257.6	3730	595
409.2	19.77	272.8	4346	693
430.4	22.21	283.9	4983	794.4
451.6	25.32	815.3	4229	685.5
472.8	25.33	251.3	5015	799.2
494.1	25.41	462.1	5143	821.8
515.3	26.01	628.4	5224	837.3
536.5	29.18	500.7	5838	932.5
557.7	29.59	665.3	5912	946.9
578.9	34.35	533.2	6914	1104
600.1	31.94	647.7	6583	1053
621.4	37.62	729.5	7639	1221
642.6	35.08	946	7044	1131
663.8	40.88	983.8	8284	1328
685	45.54	2315	1.138E4	1849
706.2	40.84	1014	8244	1322
727.4	44.11	521.8	8715	1390
748.6	56.05	1629	1.157E4	1860

769.8	61.72	1593	1.287E4	2064
791	69.22	1822	1.5E4	2404
812.2	75.57	1644	1.637E4	2619
833.4	82.1	1729	1.824E4	2917